

Chapter 2 Method of the Survey

CHAPTER 3 GEOPHYSICAL SURVEY

2-1 Outline of Survey

2 - 1 - 1 Objective

The objective of the geophysical survey is to clarify the resistivity structure and chargeability anomaly in the areas of Tempursari and Seweden, and to select proposed drilling sites by the interpretation with geological information.

2 - 1 - 2 Exploration Method

Time domain IP method

2 - 1 - 3 Amounts of Survey

Amounts of the geophysical survey are as follows.

Field survey

Total length of lines 30.2 km

Survey lines 10 lines

Measuring points 555 points

Laboratory test 21 pcs

2 - 2 Survey Method

2 - 2 - 1 Methodology

The IP is an exploration method to observe electric polarization effect (IP effect) in the earth. The IP effect is caused by the following phenomena.

When direct current flows through the rocks containing metallic minerals, electric potential difference is generated between the surface of metallic minerals and pore water around it. This electric potential causes a store of electric charge and induces electric polarization. The electric charge is discharged gradually after current is cut off. It forms the residual voltage decaying with

the passage of time. However, the IP effect occurs not only in the rocks containing metallic minerals, but also in some sedimentary rocks containing graphite or clay.

In the time domain IP method, on and off alternating current in the shape of rectangular wave, as shown in Fig. 3-1, is generally used as transmitter current. Received voltage is composed of the primary voltage V_p observed during current on and the decay voltage (secondary voltage V_s) observed during current off. Chargeability is calculated with received voltage as index to express quantity of IP effect. The chargeability M is defined in the following equation. It is the proportion of time integral of secondary voltage to primary voltage. Its unit is mV/V.

$$M = 1/V_p / (t_2 - t_1) \cdot \int_{t_1}^{t_2} V_s dt \quad (3-1)$$

t_1 : Time at the beginning of V_s integration

t_2 : Time at the end of V_s integration

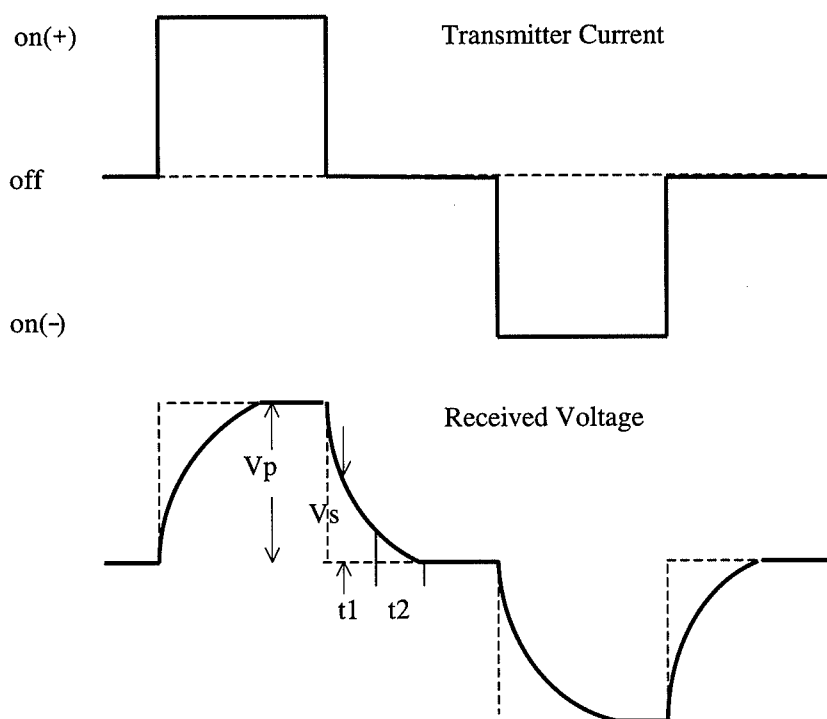


Fig.3-1 Wave Form of Transmitter Current and Received Voltage

2 - 2 - 2 Field Survey

Ten survey lines were laid out in the high mineral potential areas selected on the basis of the results of the geological survey and the soil geochemical exploration. Locations of the survey lines in the Seweden district and the Tempursari district are shown in Fig. 3-2 and Fig. 3-3 respectively. The lengths of the survey lines are shown in Table 3-1. The interval of the survey lines is 500 m.

Table 3-1 List of IP Survey Lines

Area	Line	Length [km]	Amount of Measuring Points
Seweden	1	4.0	80
	2	4.0	80
	3	4.0	80
	4	2.6	45
	5	2.6	45
	6	2.6	45
Tempursari	1	2.6	45
	2	2.6	45
	3	2.6	45
	4	2.6	45
Total		30.2	555

The specifications of the measurement are as follows.

Electrode configuration	: Dipole-dipole array
Interval of measuring points	: 200 m
Electrode separation index	: 1 to 5
Electrode spacing	: 200 m
Observed quantity	: Electric potential and chargeability
ON / OFF time	: 2 sec
Time at the beginning of Vs measurement	: 450 msec
Time at the end of Vs measurement	: 1,100 msec

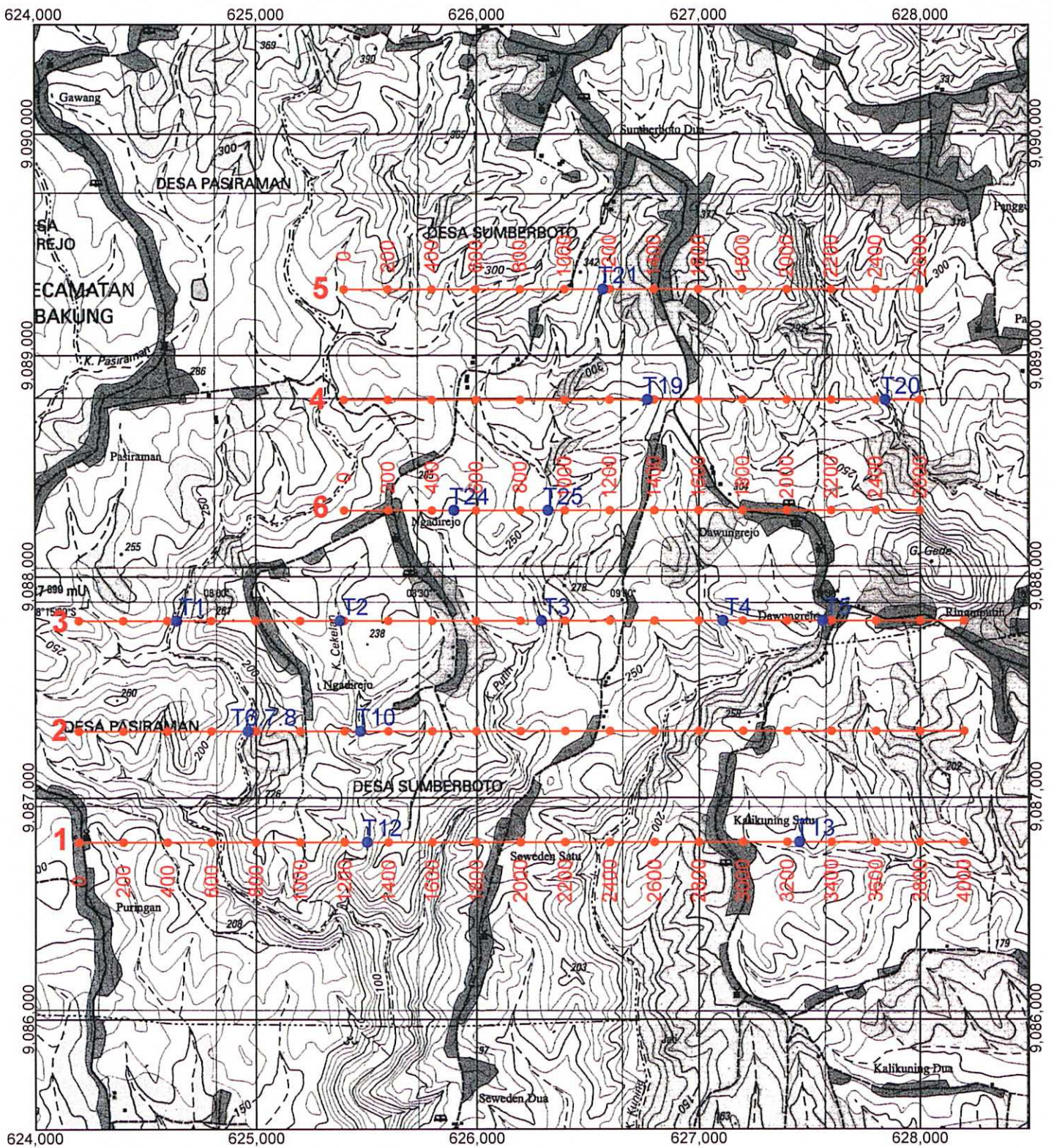
The equipment used in the IP survey is shown in Table 3-2.

Table 3-2 List of IP Survey Equipment

ITEM	MODEL	SPECIFICATION
Transmitter	Chiba CH-96T Transmitter	Output Voltage : 70, 120, 180, 250, 330, 420, 520, 630, 750, 880 V Output Current : 0~15 A
	Chiba CH-96A Power Controller	Wave Form : Rectangular Wave Frequency Range : DC~10,000 Hz Weight : 67 kg
Engine Generator	Honda ET4500 Engine Generator	Output Power : 4.5 kW Output Voltage : 200 V Weight : 78 kg
Receiver	Scintrex IPR-12 Time Domain IP/Resistivity Receiver	On/Off Time : 1, 2, 4, 8, 16, 32 s Resolution (VP) : 10 μ V Resolution (M) : 0.01 mV/V Power : 12V Battery Weight : 5.8 kg
Electrode		Current : Stainless Rod Potential : Non Polarization CuSO ₄ Porous Pot

2 - 2 - 3 Laboratory Test

Resistivity and chargeability of rock samples in the both survey areas were measured in laboratory. The same method as in the field measurement was applied. Twenty-one samples were measured in laboratory. Locations of the rock samples in the Seweden district and the Tempursari district are shown in Fig. 3-2 and Fig. 3-3 respectively.



LEGEND

- Survey Line & Measurement points
- Rock Sample Locality

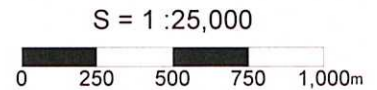


Fig.3-2 Location Map of IP Survey Lines and Rock Samples in the Seweden District

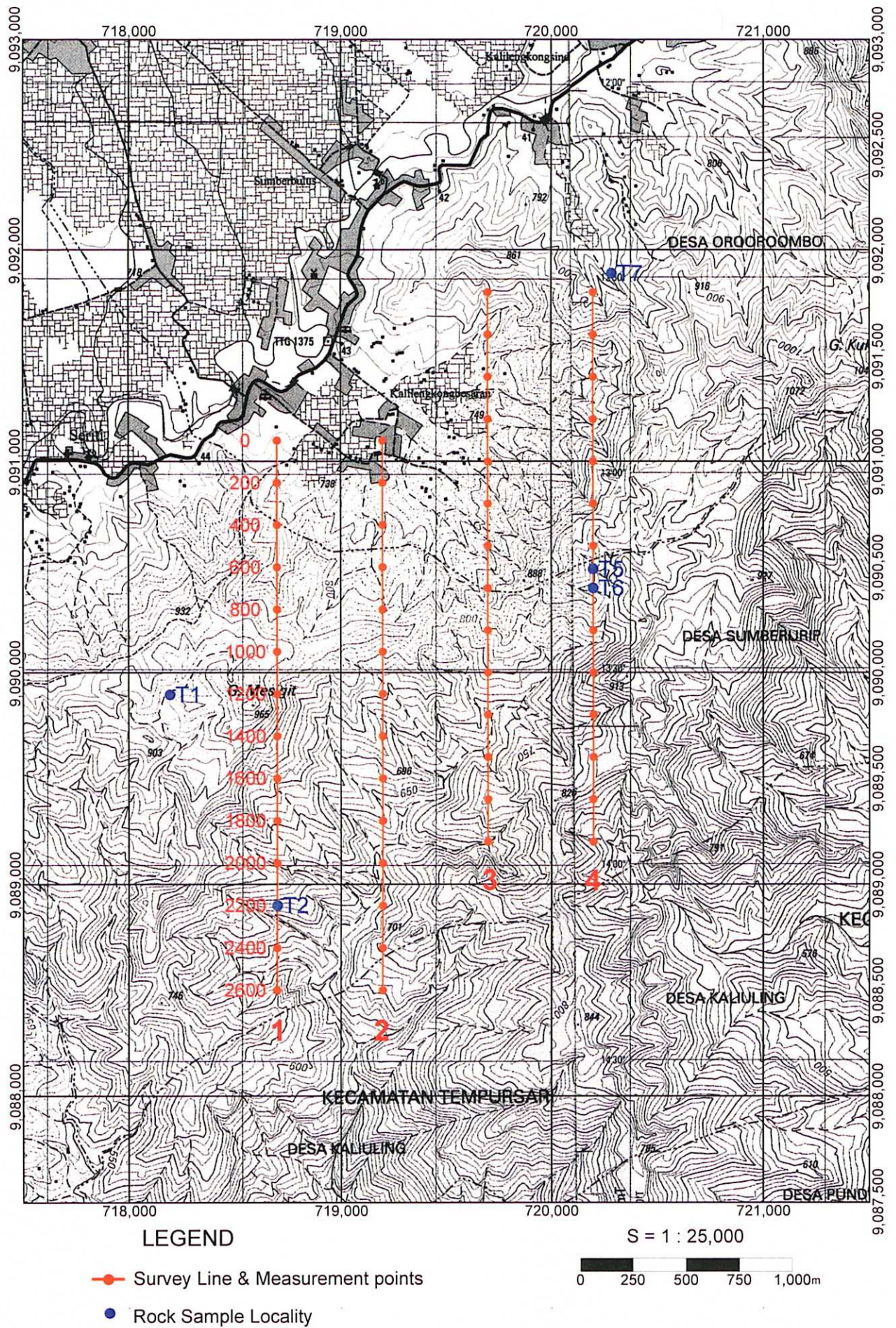


Fig.3-3 Location Map of IP Survey Lines and Rock Samples in the Tempursari District

2 - 2 - 4 Analytical Method

The analysis was carried out according to the flow chart as shown in Fig. 3-4.

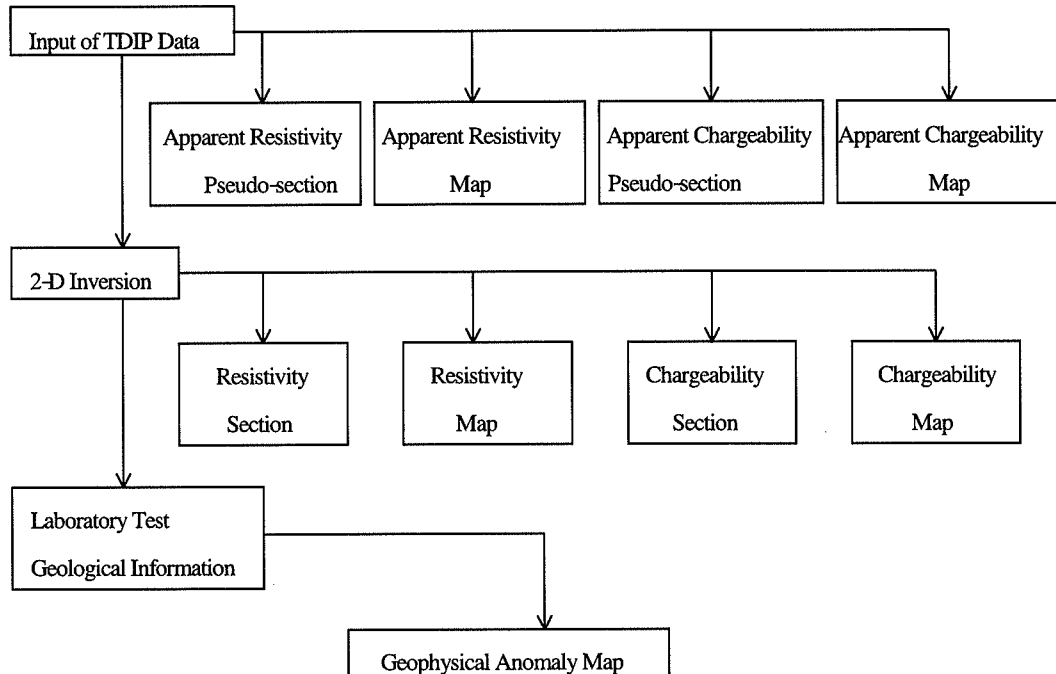


Fig.3-4 Flow Chart of the Analytical Method

(1) Apparent Resistivity Pseudo-section

In this section, apparent resistivity is plotted at the depth of $a(n+1)/2$ just under the middle point of the used electrodes for each line. In the above equation, a is electrode spacing and n is electrode separation index.

(2) Apparent Resistivity Map

In this map, the apparent resistivity of the specific electrode separation index is plotted.

(3) Apparent Chargeability Pseudo-section

In this section, apparent chargeability is plotted at the depth of $a(n+1)/2$ just under the middle point of the used electrodes for each line. In the above equation, a is electrode spacing and n is electrode separation index.

(4) Apparent Chargeability Map

In this map, the apparent chargeability of the specific electrode separation index is plotted.

(5) 2-D Inversion

This analysis assumes that structure is two dimensional, and determines the optimum resistivity distribution of two-dimensional model for each line. The distribution of apparent resistivity calculated for the optimum model is best matched to that of the observed apparent resistivity. The finite element method is applied to the forward analysis and the non-linear least squares method with smoothness constraint is applied to the optimization of resistivity distribution.

After resistivity distribution is obtained, chargeability distribution is determined with the least squares method on the assumption that an observed chargeability is weighted average value of chargeability using the sensitivities of apparent resistivity as a weighting function.

(6) Resistivity Section

In this section, the resistivity distribution below each line is drawn using the results of the 2-D inversion.

(7) Resistivity Map

In this map, the resistivity distribution at the specific level is drawn using the results of the 2-D inversion.

(8) Chargeability Section

In this section, the chargeability distribution below each line is drawn using the results of the 2-D inversion.

(9) Chargeability Map

In this map, the chargeability distribution at the specific level is drawn using the results of the 2-D inversion.

(10) Geophysical Anomaly Map

In this map, the geophysical anomalies are extracted.

2-3 Survey Results

2 - 3 - 1 Seweden District

(1) Observed Data

(a) Apparent Resistivity

The apparent resistivity pseudo-sections of six lines are shown in Fig. 3-5 and the apparent resistivity map of $n=3$ is shown in Fig. 3-6. The resistivity in this area is low on the whole, because the mean value of apparent resistivity is approximately 70 ohm-m. The resistivity trends to be higher in the northern part. Roughly speaking, the resistivity of the southern three lines ranges from 20 to 100 ohm-m, and the resistivity of the northern three lines ranges from 50 to 200 ohm-m.

(b) Apparent Chargeability

The apparent chargeability pseudo-sections of six lines are shown in Fig. 3-7 and the apparent chargeability map of $n=3$ is shown in Fig. 3-8. The background value of chargeability in the area seems to be about 10 mV/V, judging from the apparent chargeability. The chargeability trends to be higher in the eastern parts of line-2 and line-3, and to decrease northward and westward. The chargeability anomalies exceeding 30 mV/V are detected in the eastern deep parts of line-2 and line-3.

(2) Analytic Results

(a) Resistivity

The resistivity sections drawn with the 2-D inversion are shown in Fig. 3-9. The resistivity maps of 2 levels (SL 100 m and SL -100 m) are shown in Fig. 3-10 and Fig. 3-11 respectively. The resistivity in the area trends to be lower in the southeastern part and to be higher in the northwestern part. Rocks in the area would be widely altered because the low resistivities of the order of 10 ohm-m distribute throughout almost whole survey area, except northwestern part and partial deep zones.

(b) Chargeability

The chargeability sections drawn with the 2-D inversion are shown in Fig. 3-12. The chargeability maps of 2 levels (SL 100 m and SL -100 m) are shown in Fig. 3-13 and Fig. 3-14 respectively. Chargeability anomalies can be outlined clearly by the 2-D inversion. The chargeability in the area trends to be higher in the central-eastern part and to be lower in the

western part, and higher in the deep zone and lower in the shallow zone. Some chargeability anomalies exceeding 30 mV/V are detected in the central-eastern deep parts of line-1, line-2, line-3 and line-4. They form two north-south trending anomalous zones on the chargeability map of SL -100 m. The chargeabilities around station 2400 and station 3200 of line-3 exceed 50 mV/V. These anomalous zones distribute in the low resistivity zone.

2 - 3 - 2 Tempursari District

(1) Observed Data

(a) Apparent Resistivity

The apparent resistivity pseudo-sections of four lines are shown in Fig. 3-15 and the apparent resistivity map of $n=3$ is shown in Fig. 3-16. The resistivity in this area is generally from 50 ohm-m to 500 ohm-m, and its average is approximately 180 ohm-m. The resistivity is higher and more changeful in this district than the Seweden district.

(b) Apparent Chargeability

The apparent chargeability pseudo-sections of four lines are shown in Fig. 3-17 and the apparent chargeability map of $n=3$ is shown in Fig. 3-18. The chargeability in the area is relatively high, since the mean value of apparent chargeability is about 18 mV/V. The chargeability trends to be higher in line-2, and to decrease eastward and northward. The chargeability anomalies exceeding 30 mV/V distribute V-shape and inverse V-shape in the sections of line-1 and line-2 respectively.

(2) Analytic Results

(a) Resistivity

The resistivity sections drawn with the 2-D inversion are shown in Fig. 3-19. The resistivity maps of 2 levels (SL 600 m and SL 400 m) are shown in Fig. 3-20 and Fig. 3-21 respectively. The resistivity in the area is generally more than 100 ohm-m and partially more than 500 ohm-m. The low resistivity zones of less than 100 ohm-m distribute in the northern parts of line-3 and line-4, and southern shallow to middle deep parts of line-1, line-2 and line-3. The latter zone extends SW-NE direction on the resistivity map of SL 400 m.

(b) Chargeability

The chargeability sections drawn with the 2-D inversion are shown in Fig. 3-22. The chargeability maps of 2 levels (SL 600 m and SL 400 m) are shown in Fig. 3-23 and Fig. 3-24,

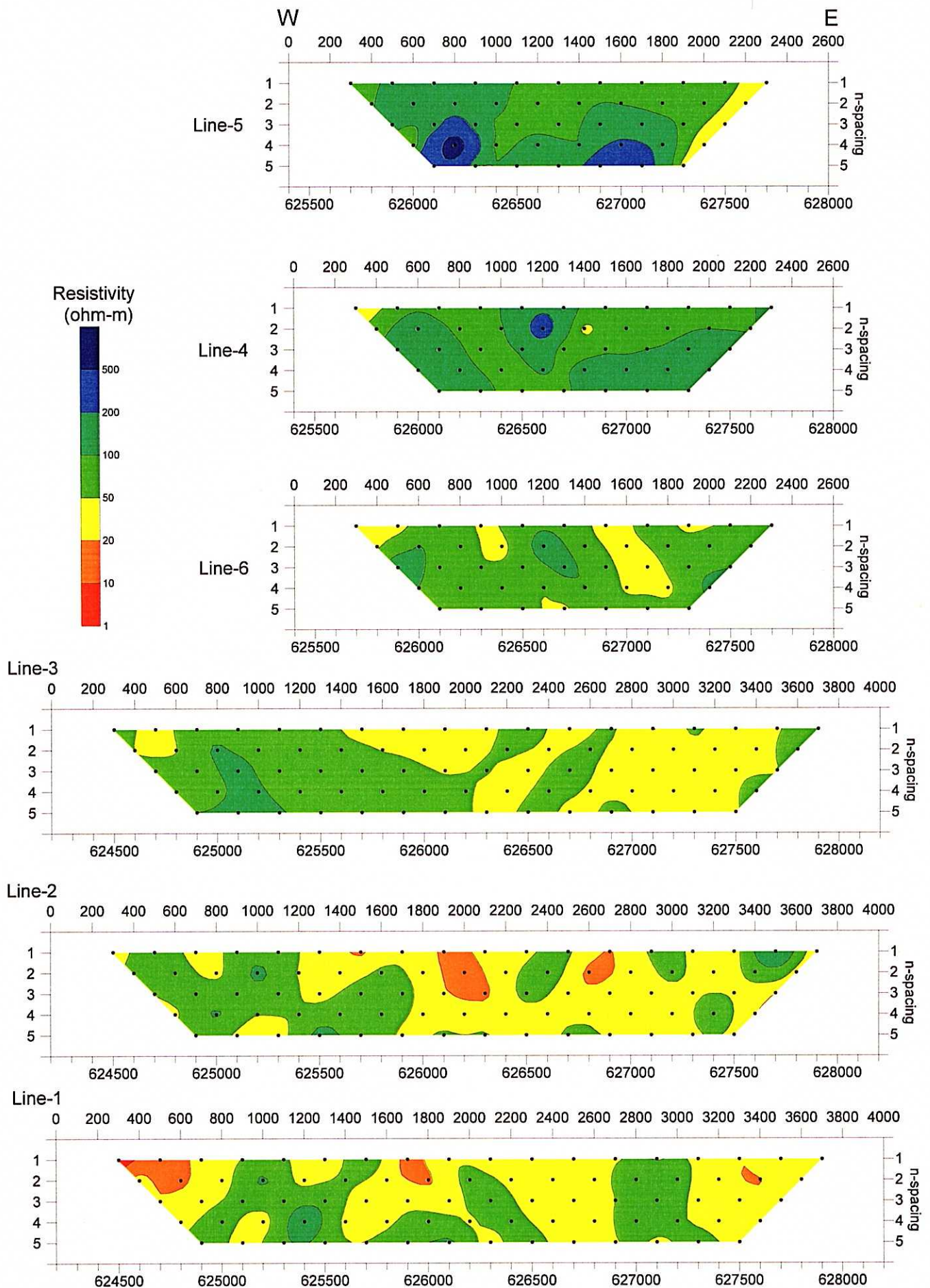


Fig.3-5 Apparent Resistivity Pseudo-sections of the Seweden District

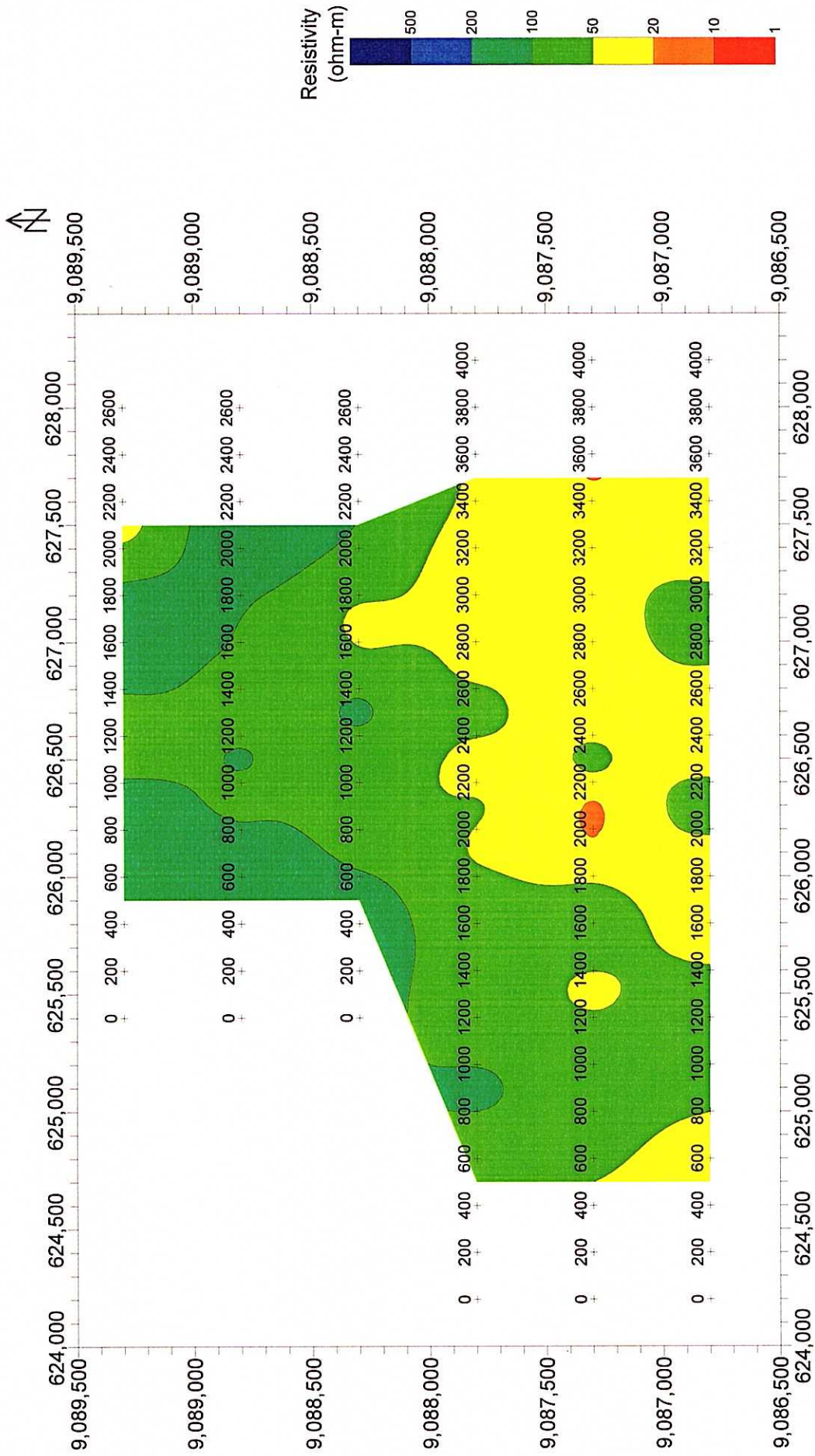


Fig.3-6 Apparent Resistivity Map of the Seweden District (n=3)

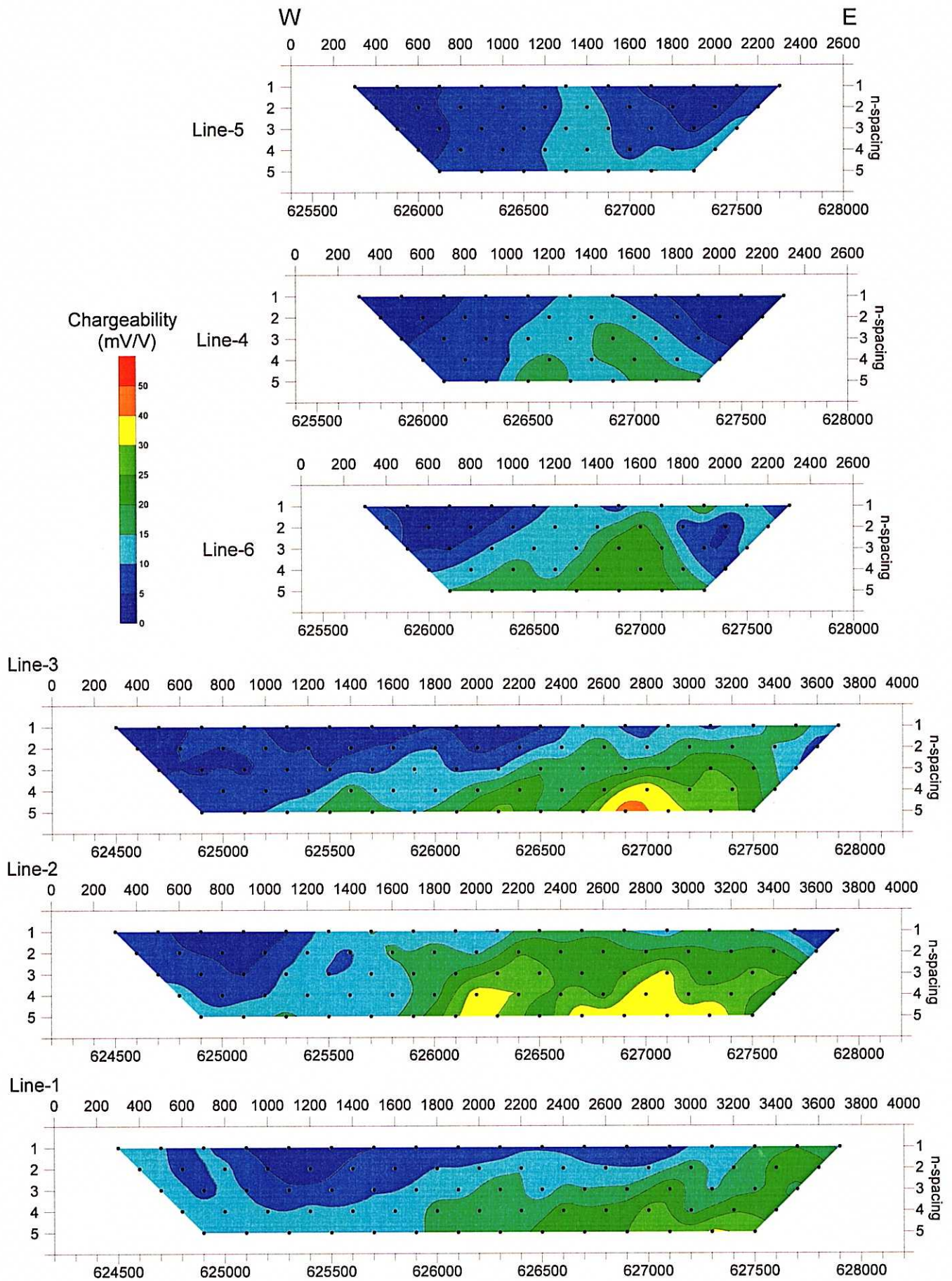


Fig.3-7 Apparent Chargeability Pseudo-sections of the Seweden District

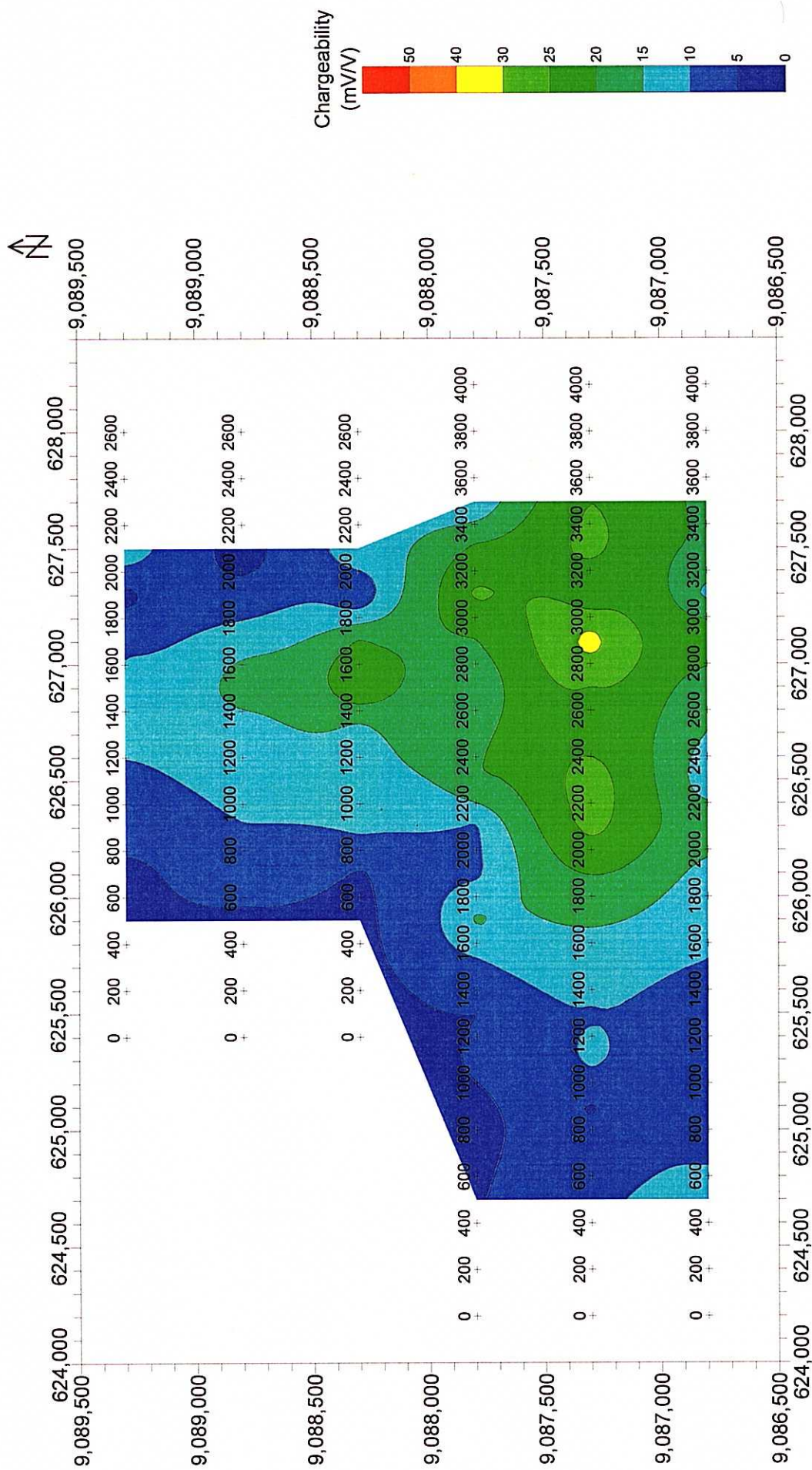


Fig.3-8 Apparent Chargeability Map of the Seweden District (n=3)

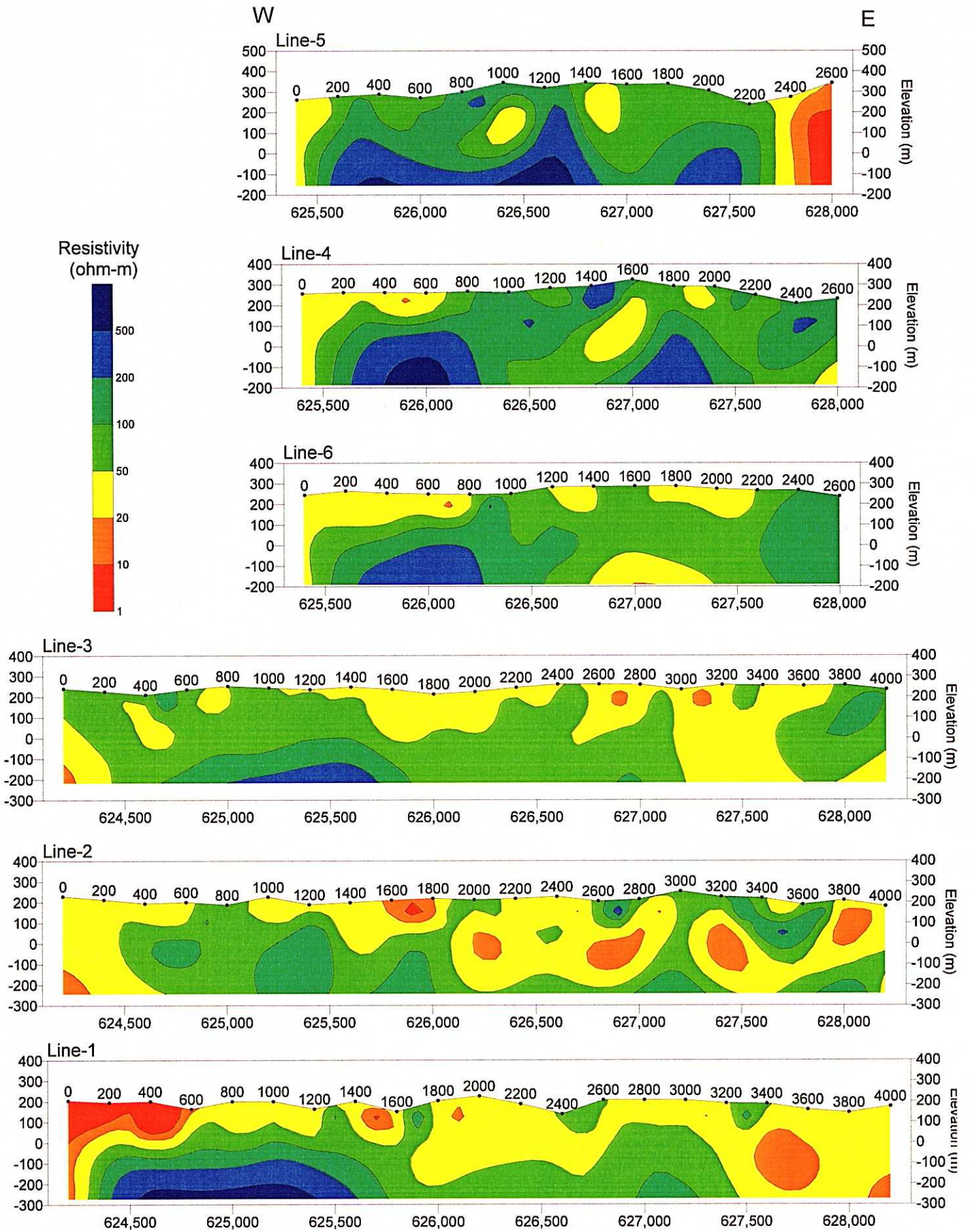


Fig.3-9 Resistivity Sections of the Seweden District

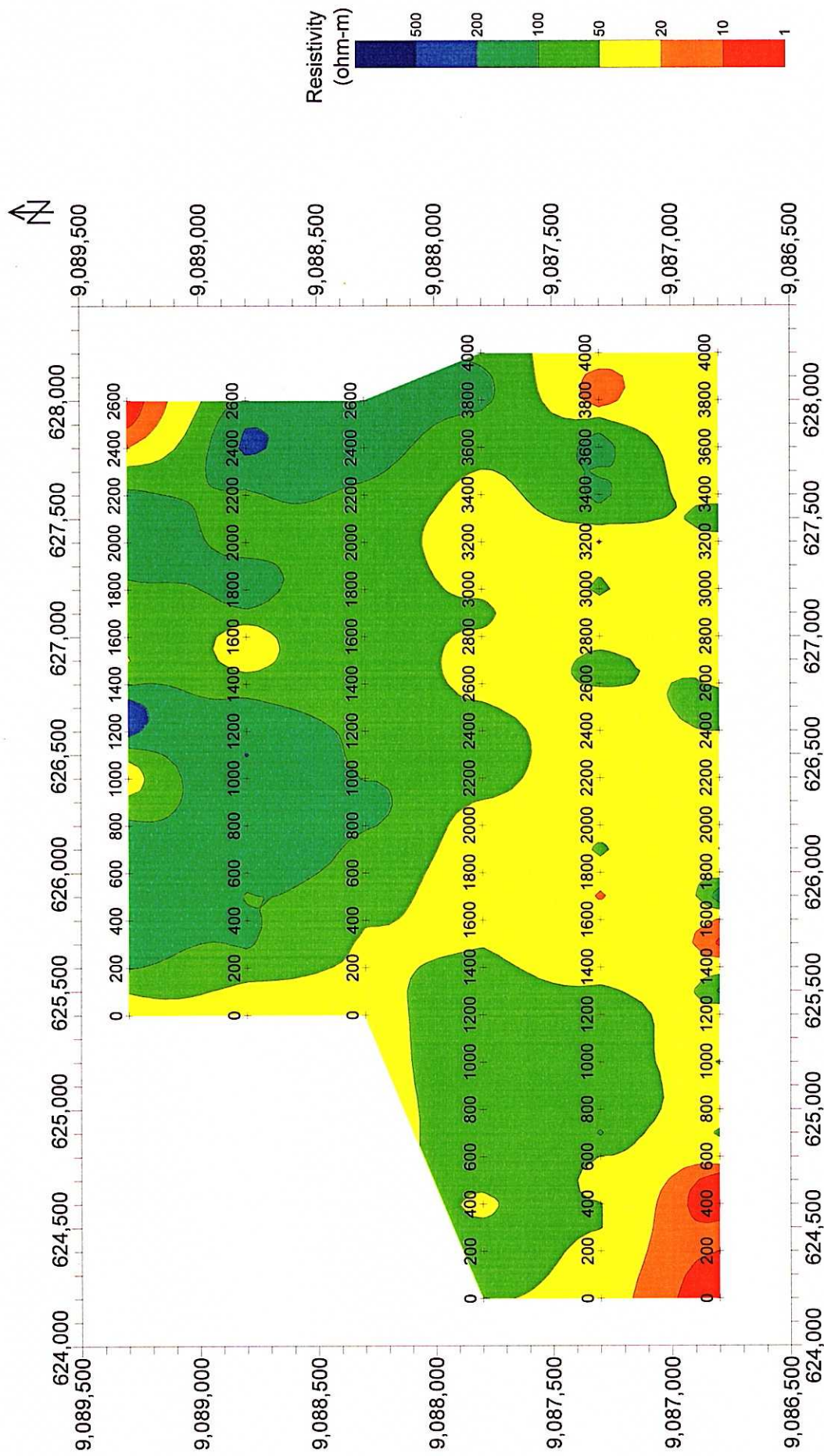


Fig.3-10 Resistivity Map of the Seweden District (SL=100m)

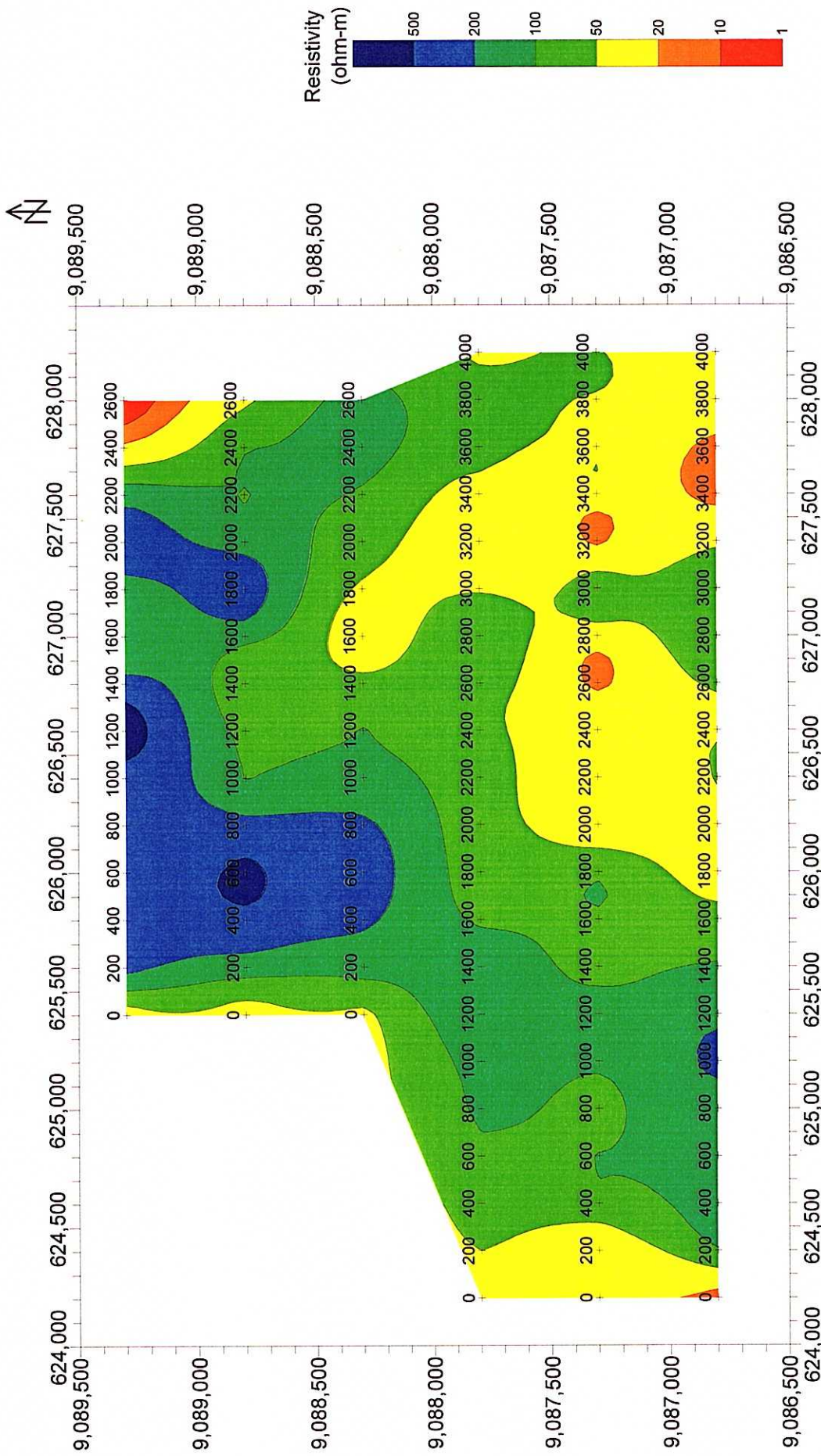


Fig.3-11 Resistivity Map of the Seweden District (SL=-100m)

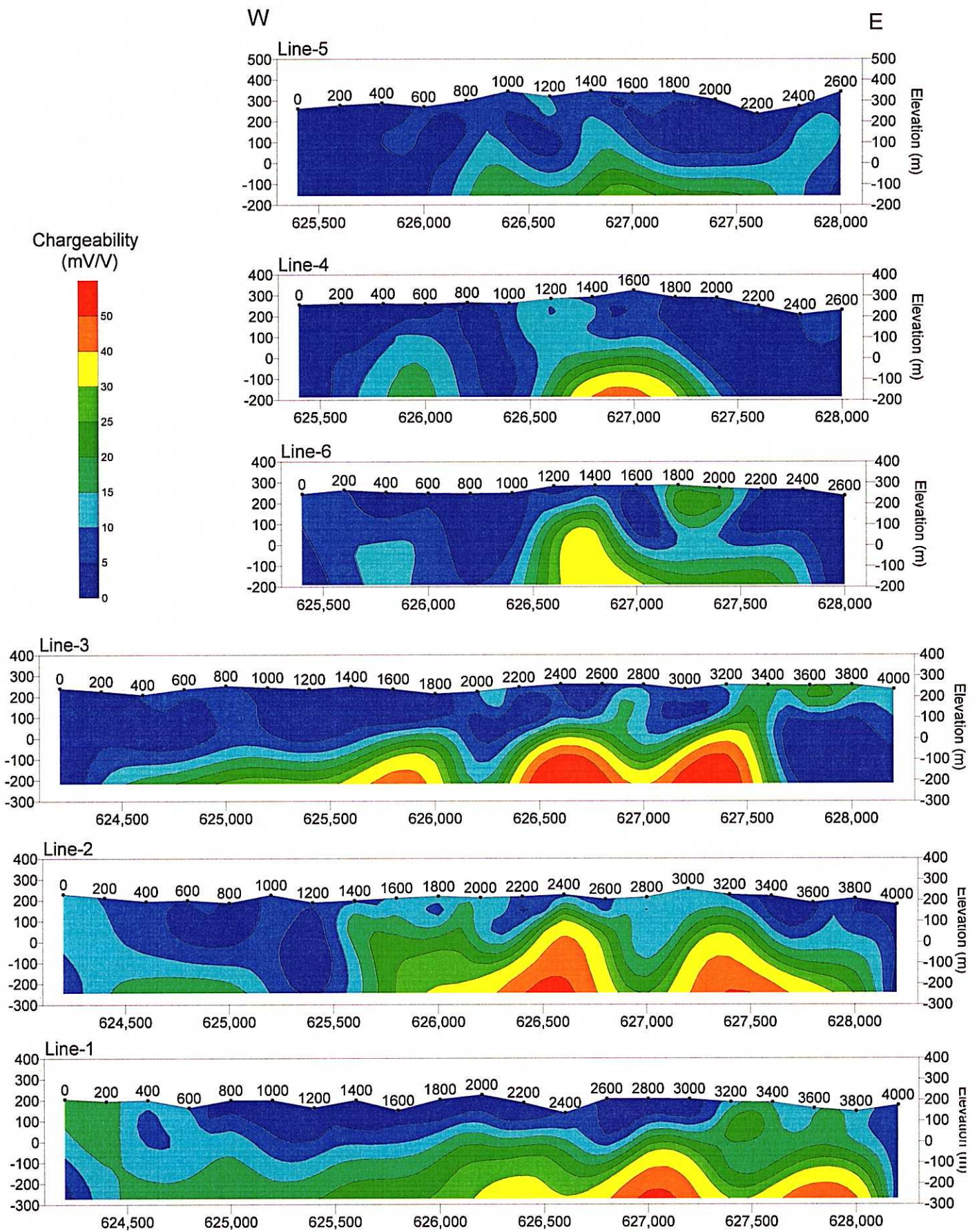


Fig.3-12 Chargeability Sections of the Seweden District

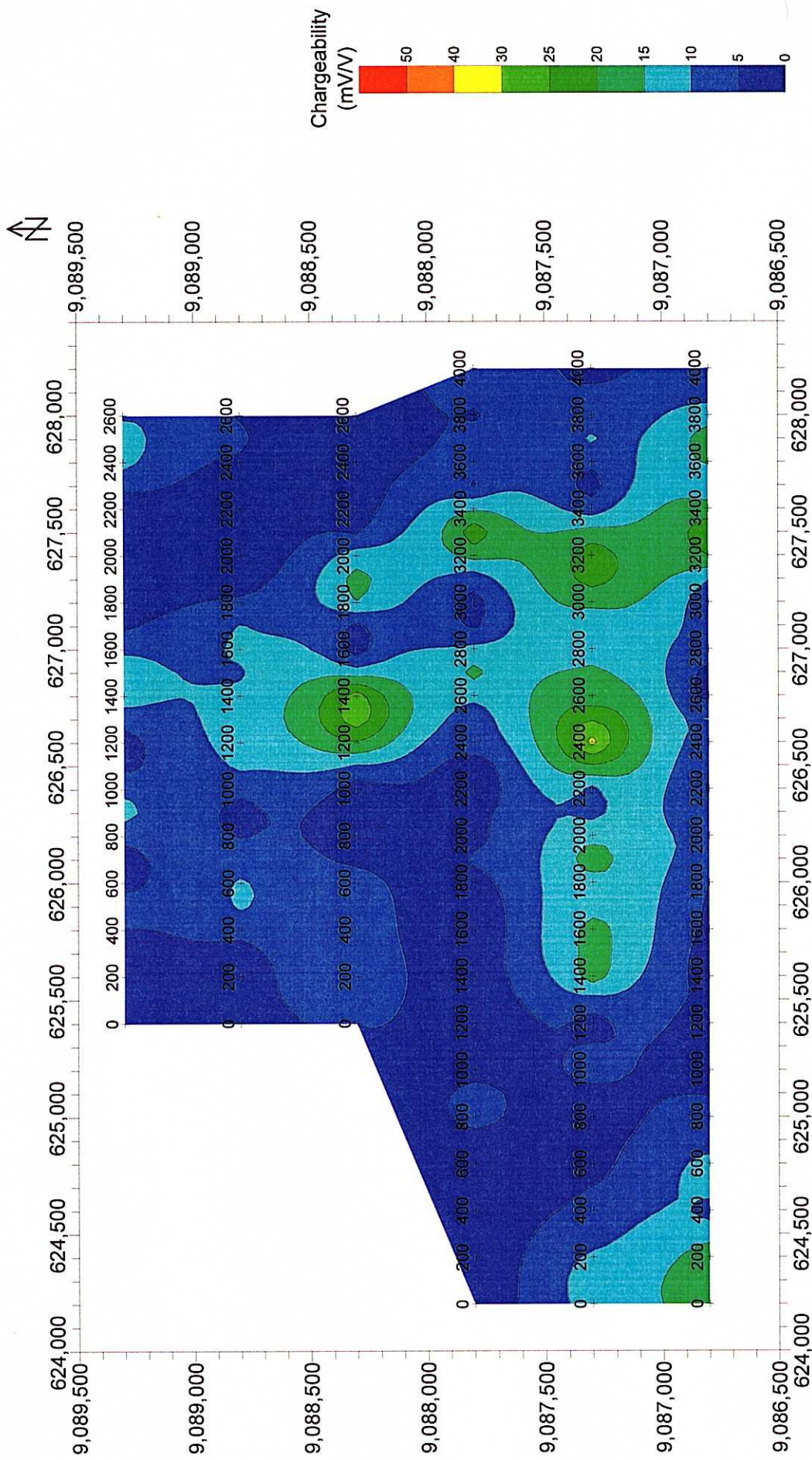


Fig.3-13 Chargeability Map of the Seweden District (SL=100m)

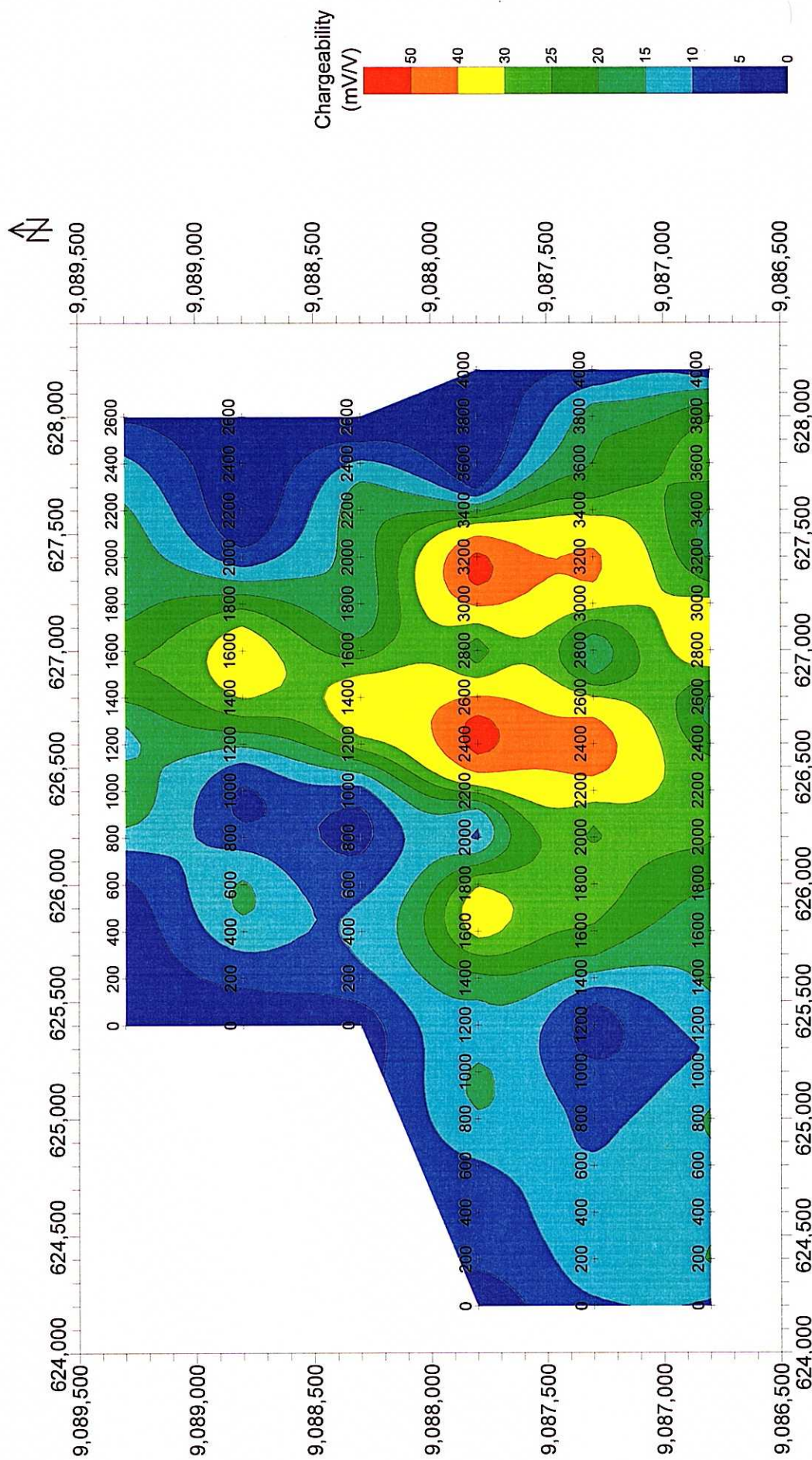


Fig.3-14 Chargeability Map of the Seweden District (SL=-100m)

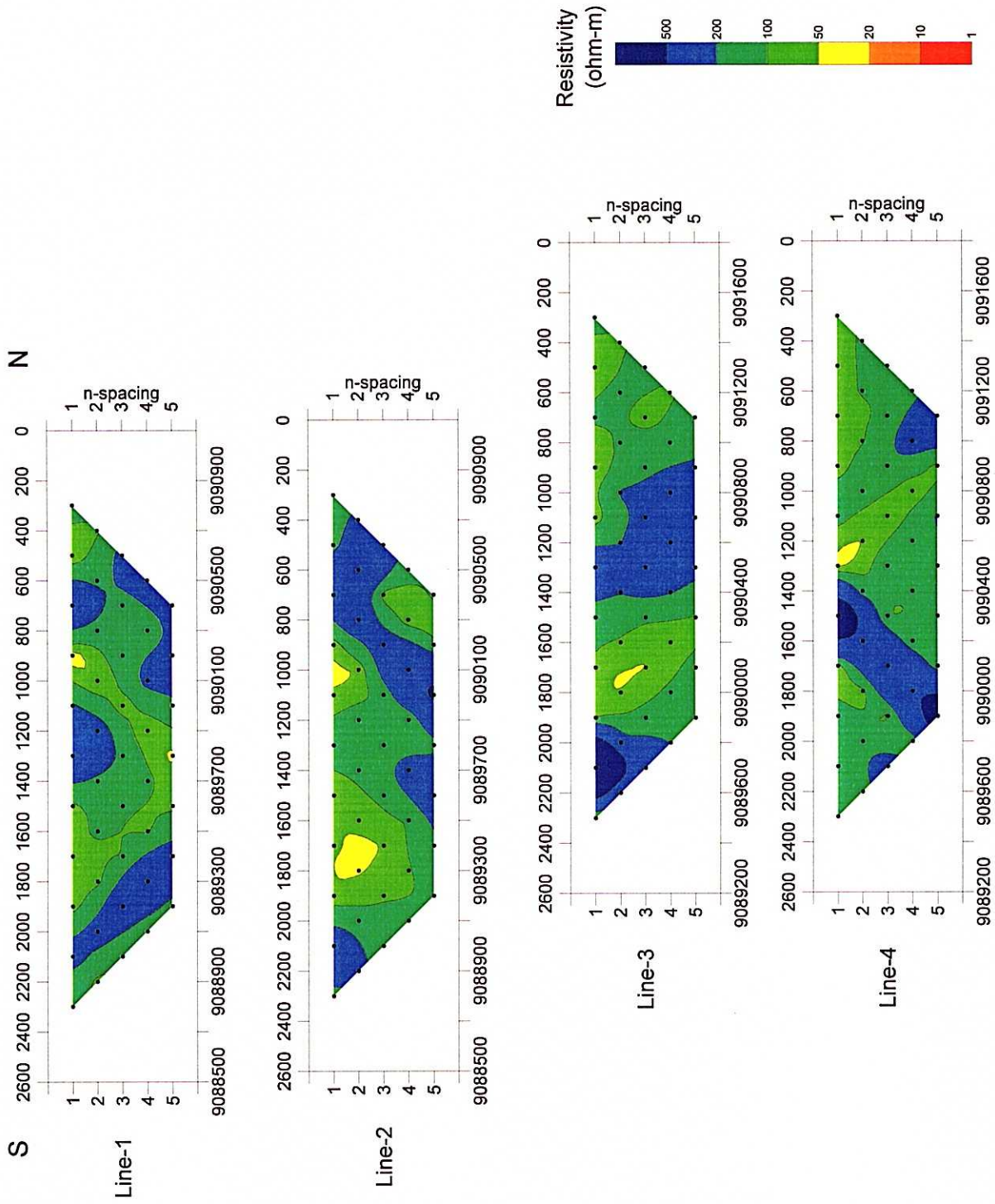


Fig.3-15 Apparent Resistivity Pseudo-sections of the Tempursari District

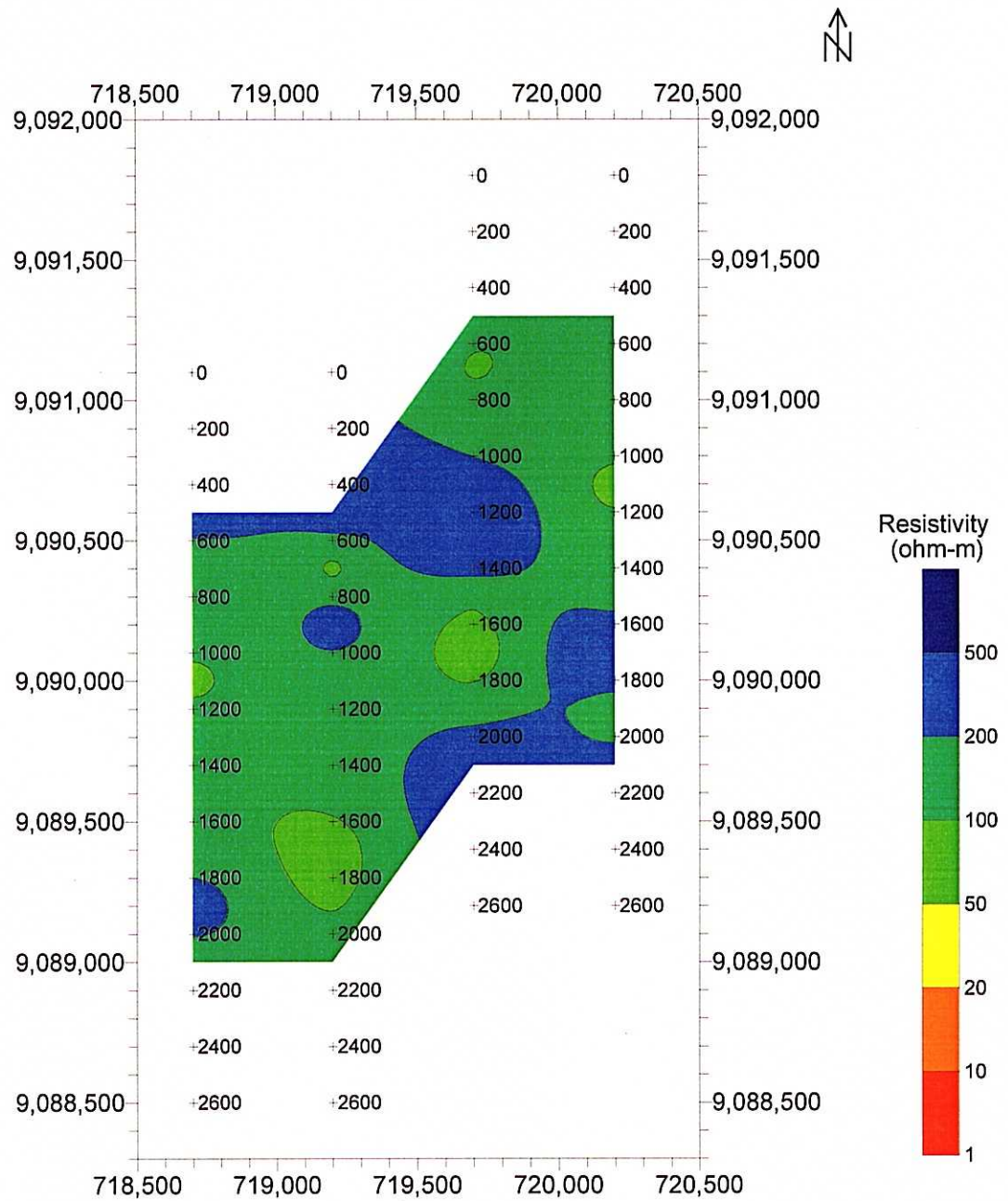


Fig.3-16 Apparent Resistivity Map of the Tempursari District (n=3)

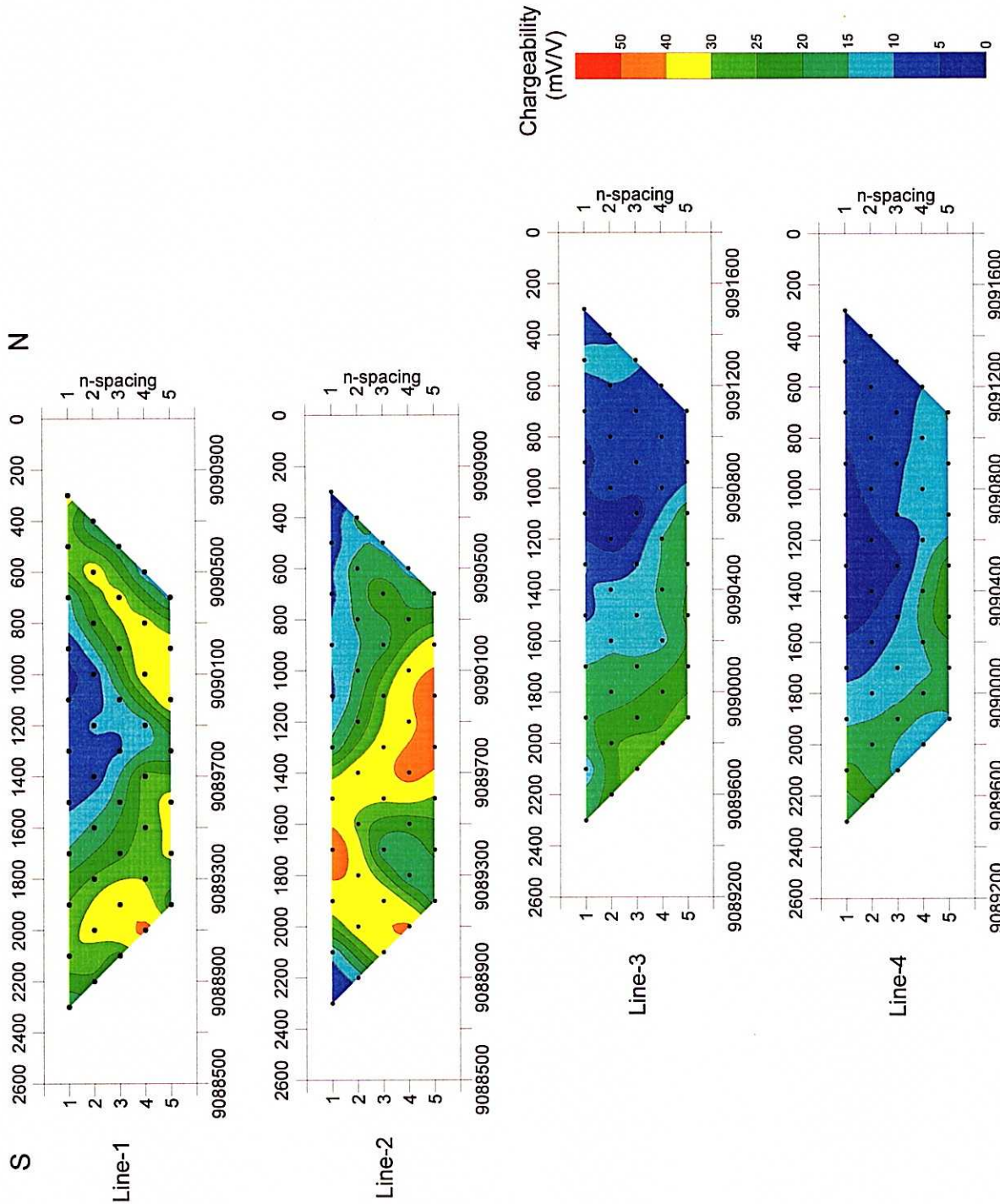


Fig.3-17 Apparent Chargeability Pseudo-sections of the Tempursari District

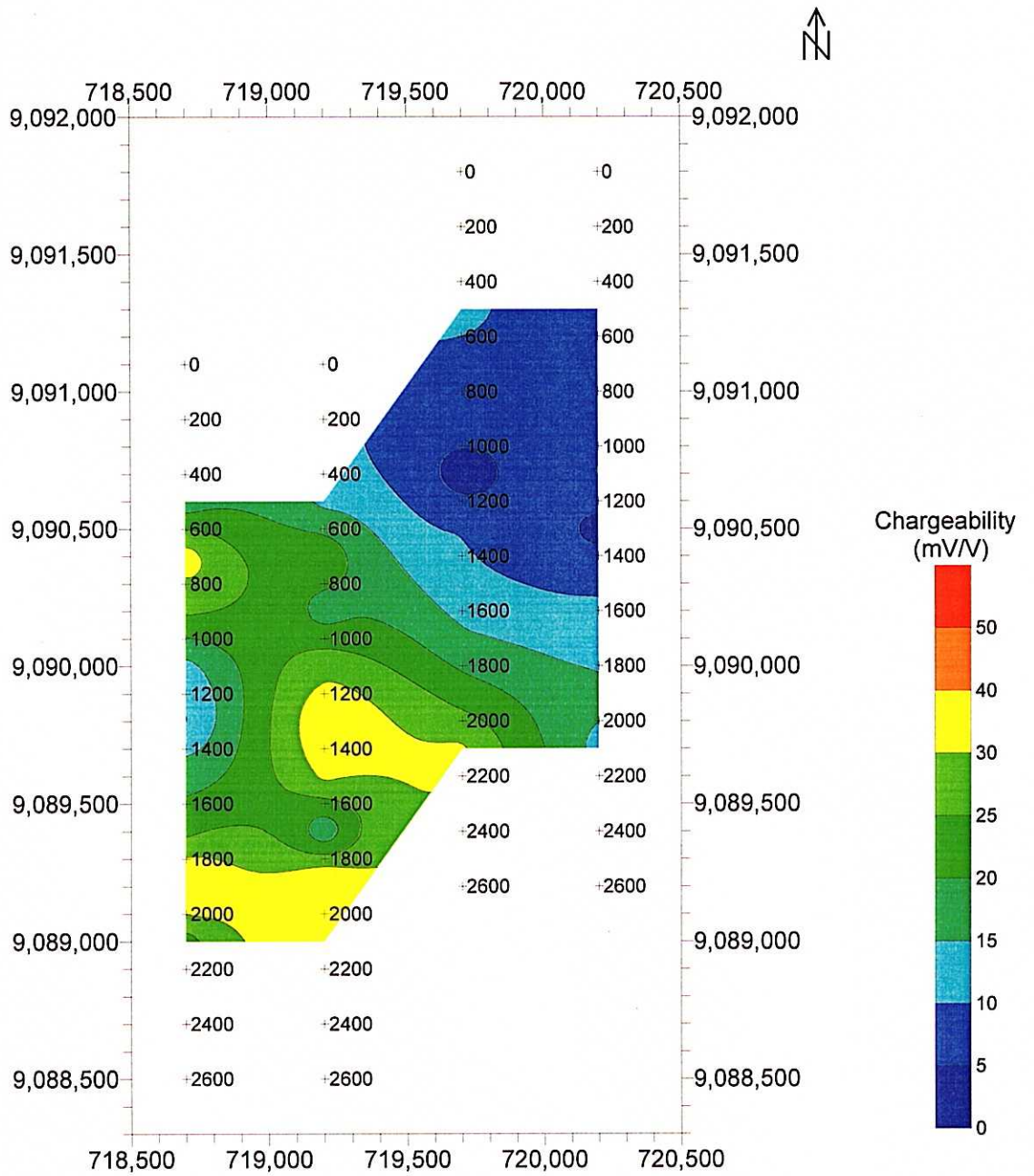


Fig.3-18 Apparent Chargeability Map of the Tempursari District (n=3)

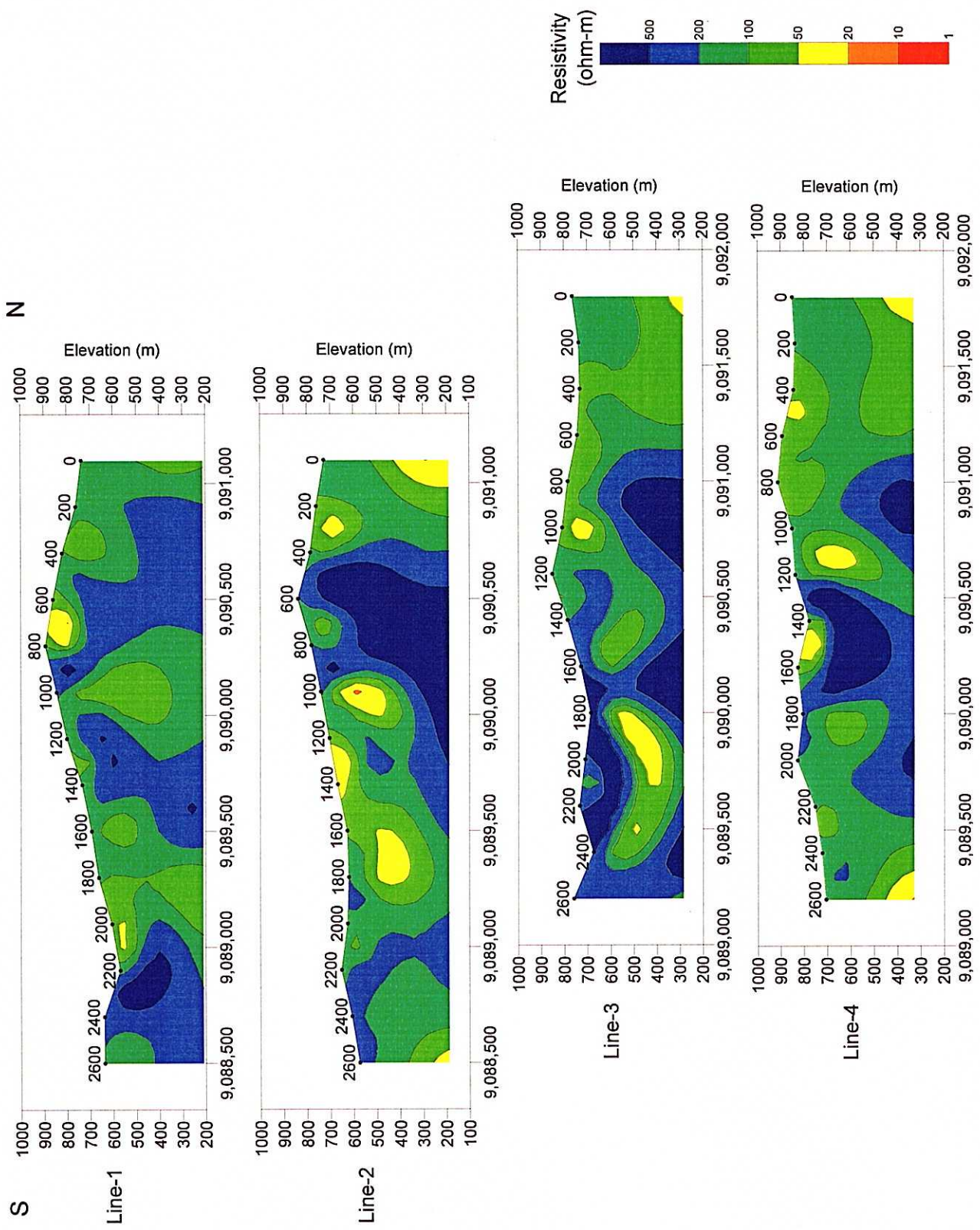


Fig.3-19 Resistivity Sections of the Tempursari District

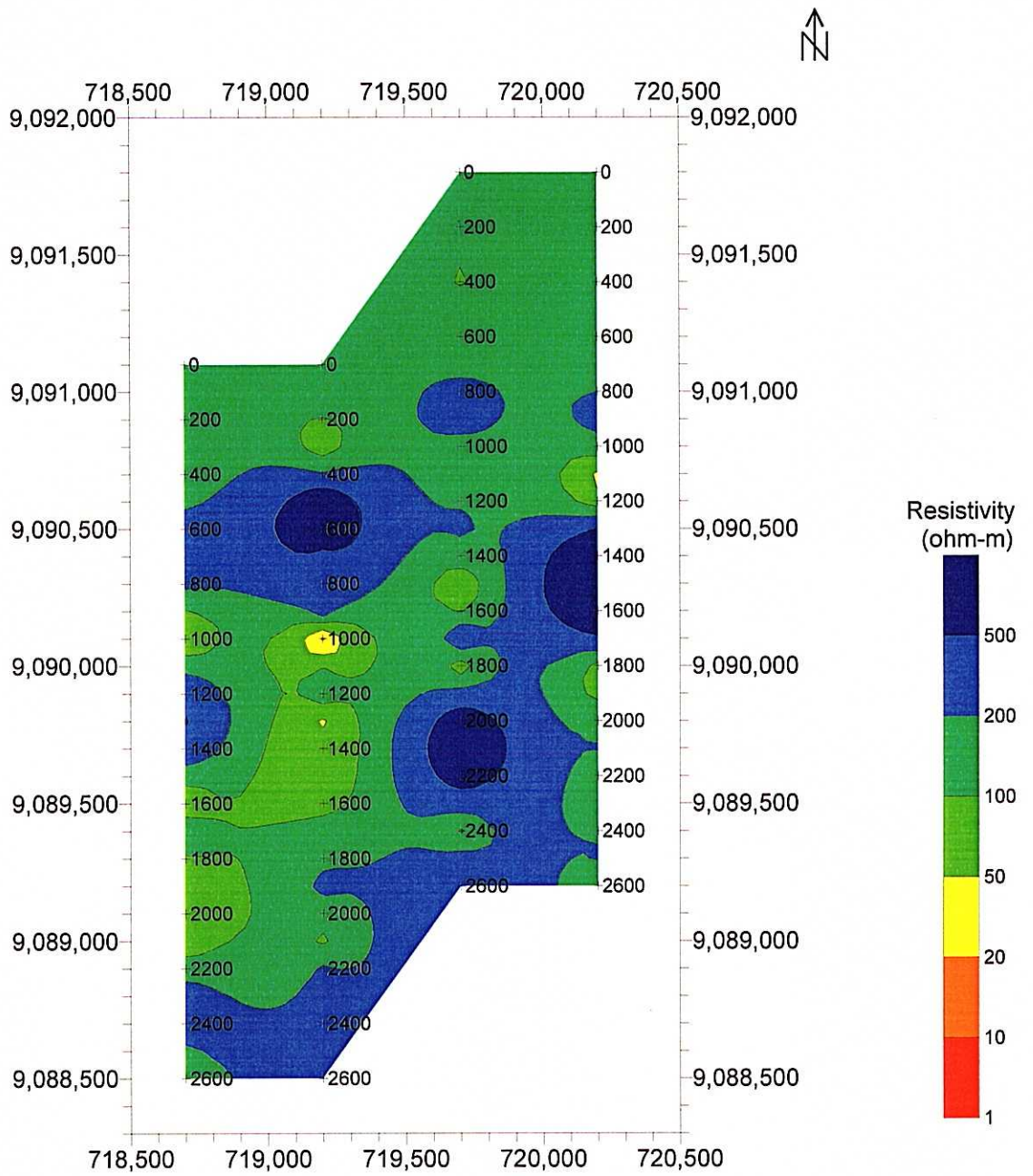


Fig.3-20 Resistivity Map of the Tempursari District (SL=600m)

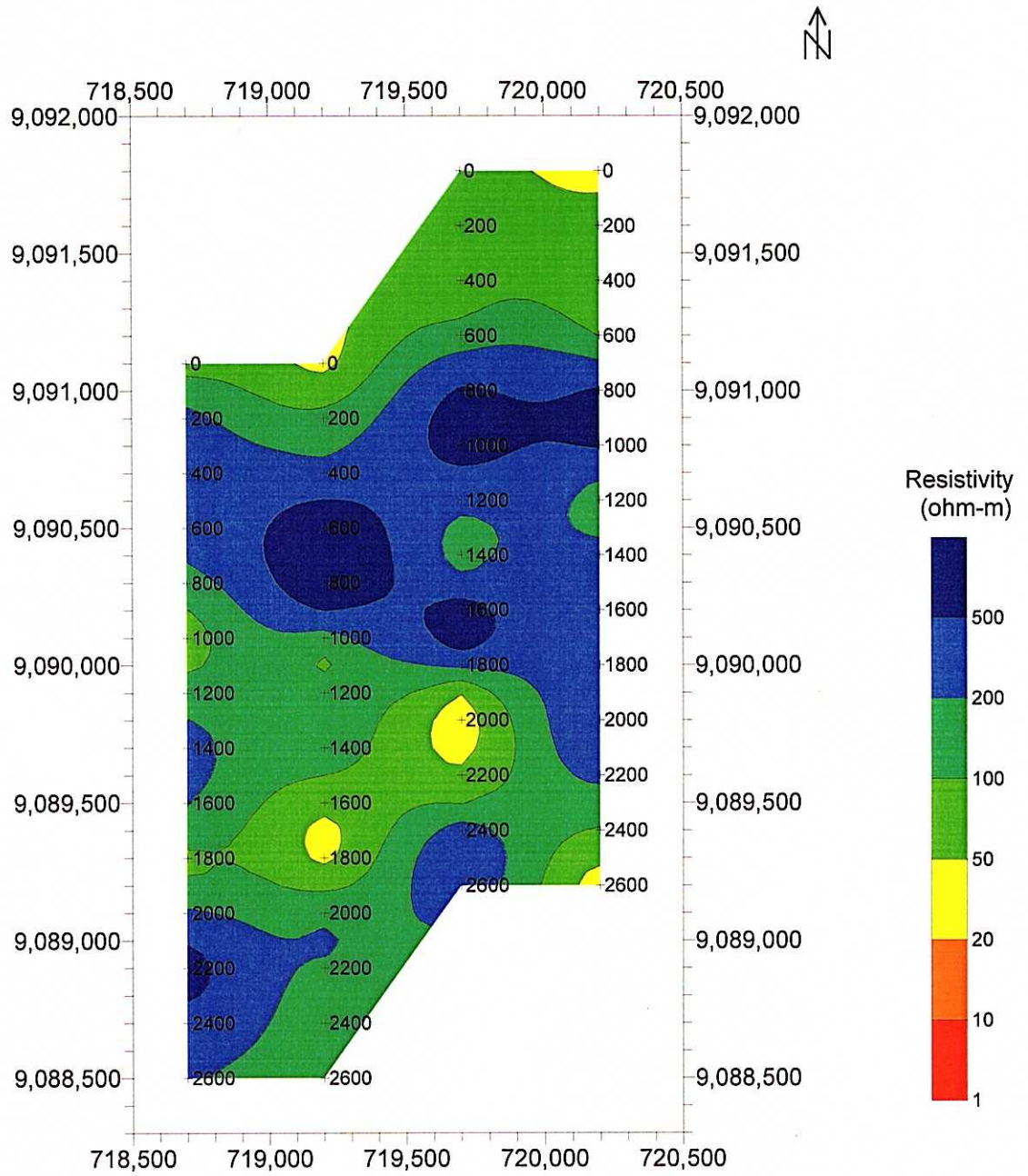


Fig.3-21 Resistivity Map of the Tempursari District (SL=400m)

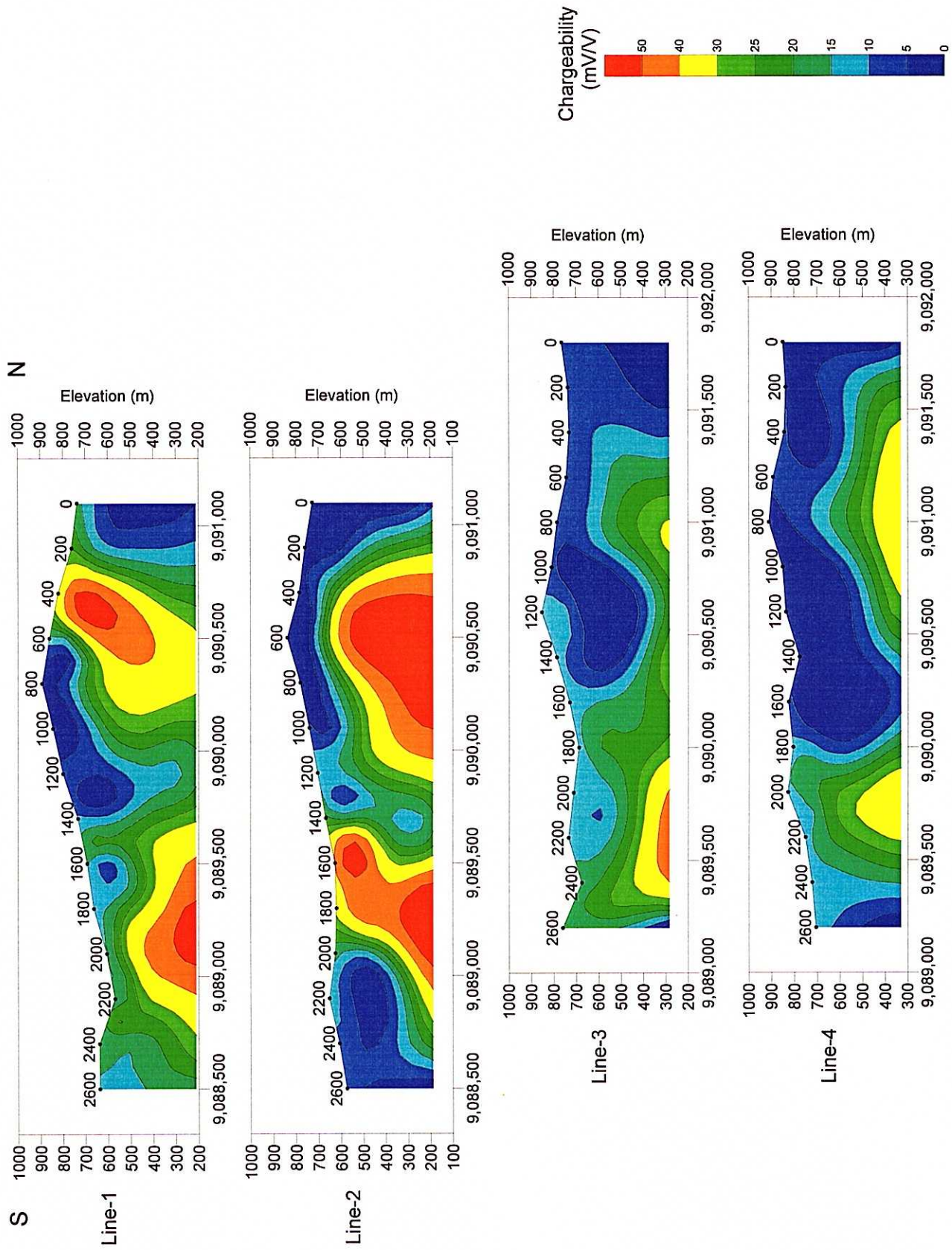


Fig.3-22 Chargeability Sections of the Temprusari District

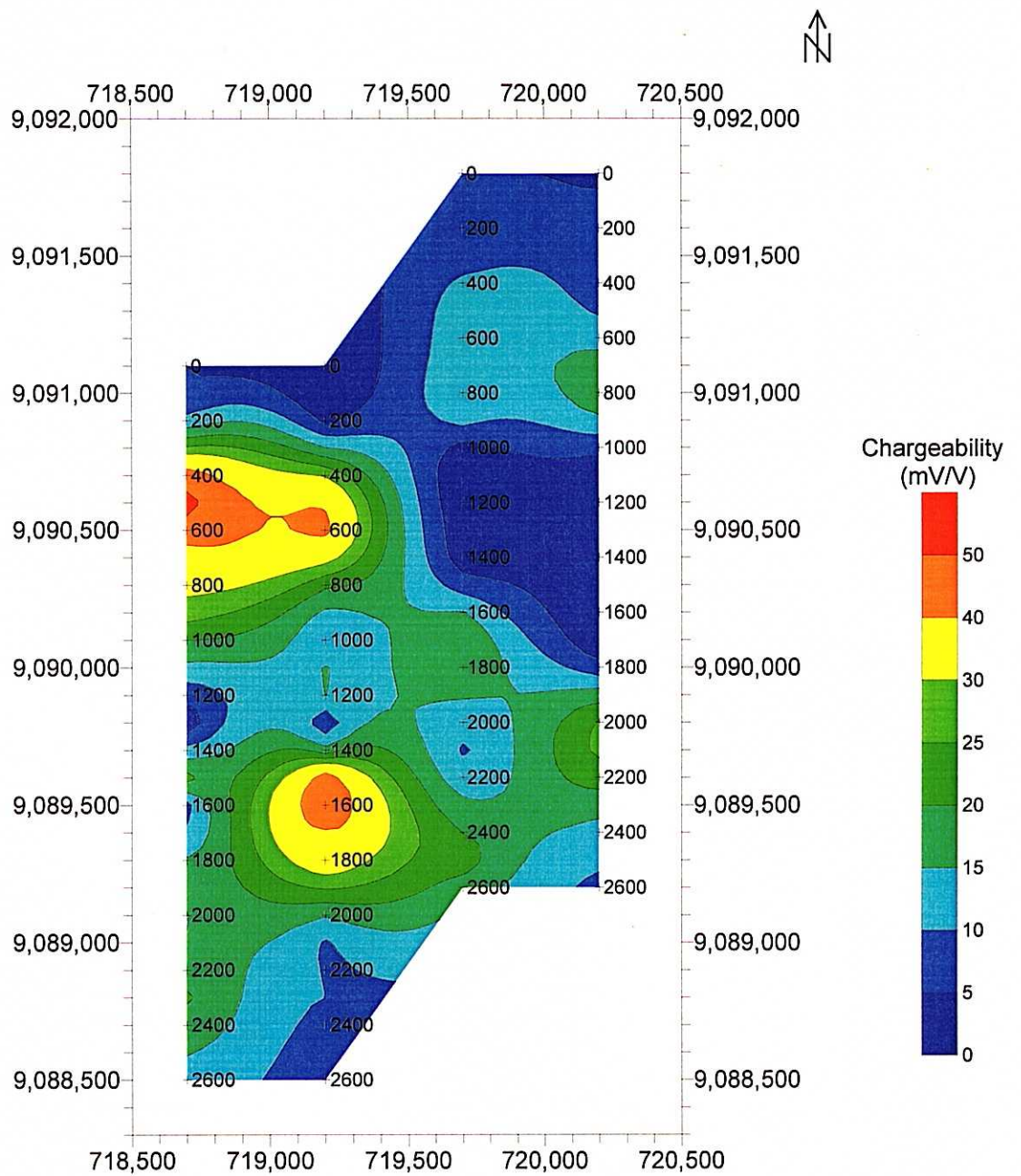


Fig.3-23 Chargeability Map of the Tempursari District (SL=600m)

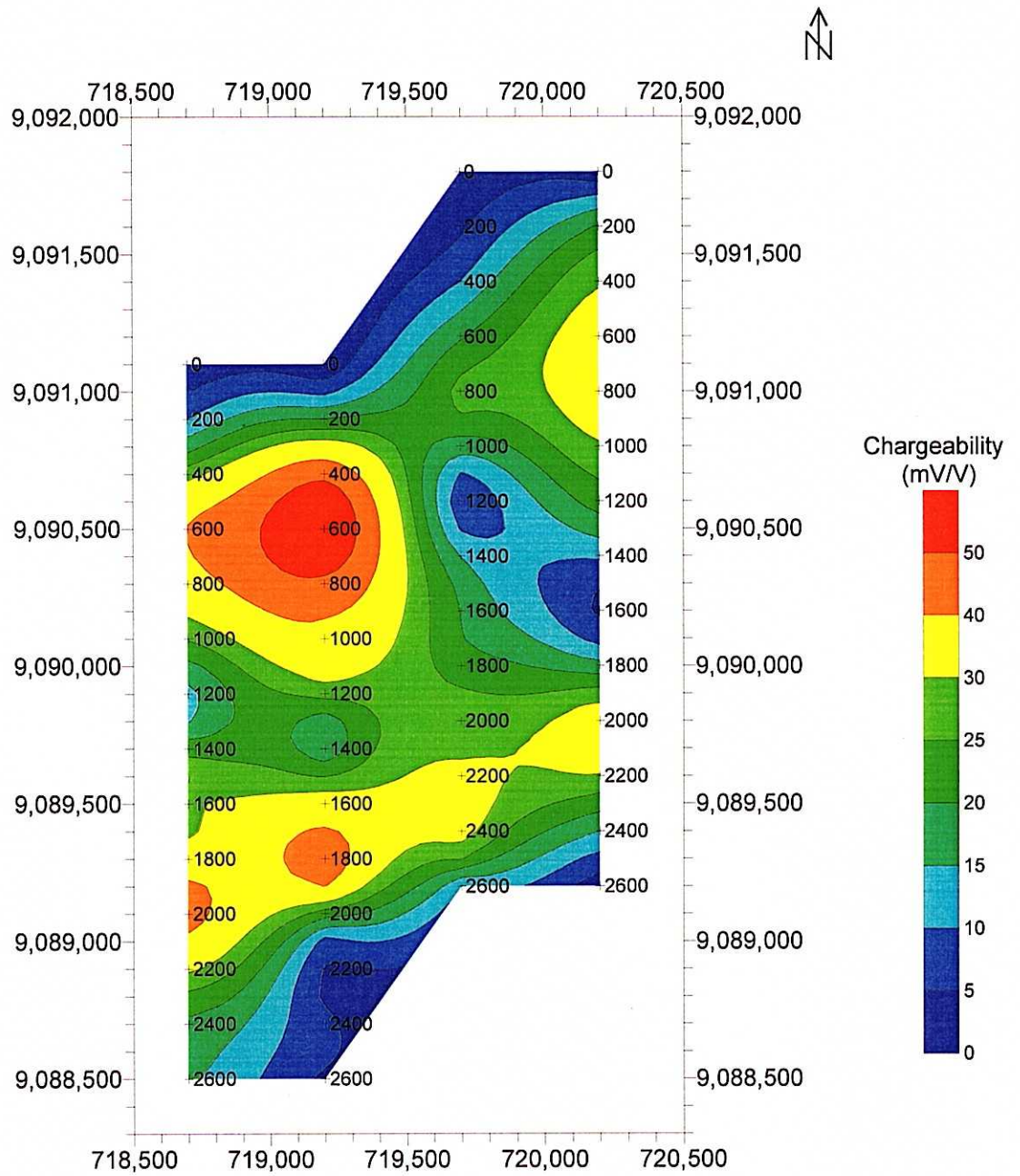


Fig.3-24 Chargeability Map of the Tempursari District (SL=400m)

respectively. Chargeability anomalies can be outlined clearly by the 2-D inversion. The chargeability in the area trends to be higher in the western part and to be lower in the eastern part. Some chargeability anomalies exceeding 30 mV/V are detected in all four survey lines. They form two anomalous zones centered in around station 600 and station 1800 of line-2 on the chargeability map of SL 400 m. The former zone has the highest chargeability of exceeding 50 mV/V. Both anomalous zones show vertical structure.

2 - 3 - 3 Laboratory Test

The result of the laboratory test is shown in Table 3-4. The mean values of resistivity and chargeability of main rocks in both survey areas of Seweden and Tempursari are as follows.

Area	Rock	No. of Sample	Resistivity [ohm-m]	Chargeability [mV/V]
Seweden	Limestone	2	16,200	7
	Tuff	3	220	22
	Tuff breccia (silicified)	5	900	12
	Tuff breccia (argillized)	2	80	29
	Andesitic rock	4	750	12
Tempursari	Tuff breccia	3	930	21
	Andesite	2	350	18
	(Pyrite disseminated rock)	6	590	19
	(Altered rock)	4	160	21

Rocks excepting limestone and argillized tuff breccia in the survey areas generally show resistivity of 100 to 1,000 ohm-m and chargeability of 10 to 20 mV/V. These properties are not so different characteristically among these rocks. Limestone has high resistivity more than a few 1,000 ohm-m and low chargeability less than 10 mV/V. Argillized tuff breccia has low resistivity less than 100 ohm-m and high chargeability more than 20 mV/V, while silicified tuff breccia shows high resistivity and low chargeability. Tuff breccia and andesitic rocks with pyrite dissemination have higher chargeability than that without pyrite dissemination, but resistivities of those rocks are not different distinctly. The ore sample containing a large amount of pyrite may show lower resistivity. Altered rocks are characterized by low resistivity and high chargeability.

Table 3-4 Results of Laboratory Test

Sample No.	Area	Location	Rock Name	Remarks	Resistivity [ohm-m]	Chargeability [mV/V]
S12	Seweden	Line1:1300m	Limestone	Hard	2,314	12.5
S24	Seweden	Line6:500m	Limestone		30,086	0.7
S2	Seweden	Line3:1250m	Fine tuff	Weak alteration	62	27.0
S5	Seweden	Line3:3300m	Tuff	Silicified	370	17.1
S13	Seweden	Line1:3200m	Tuff	Silicified, Altered	231	21.7
S1	Seweden	Line3:500m	Tuff breccia	Silicified	2,759	5.5
S4	Seweden	Line3:2900m	Tuff breccia	Silicified	847	4.7
S6	Seweden	Line2:750m	Tuff breccia	Silicified, Py disseminated	240	15.6
S7	Seweden	Line2:750m	Tuff breccia	Silicified, Py disseminated	509	13.2
S19	Seweden	Line4:1400m	Tuff breccia	Silicified, Weak alteration	123	19.2
S3	Seweden	Line3:2100m	Tuff breccia	Clayey, Silicified	99	15.5
S10	Seweden	Line2:1250m	Tuff breccia	Clayey, Weak silicified	59	42.5
S8	Seweden	Line2:750m	Propylite	Py disseminated	152	13.1
S21	Seweden	Line5:1200m	Propylite	Py disseminated	375	13.4
S20	Seweden	Line4:2400m	Andesite	Silicified, Py disseminated	2,246	5.0
S25	Seweden	Line6:900m	Dacite	Altered	205	16.0
T1	Tempursari	West of Line1	Tuff breccia	Non alteration	822	10.9
T2	Tempursari	Line1:2200m	Tuff breccia	Py disseminated	1,716	44.3
T5	Tempursari	Line4:1300m	Tuff breccia	Non alteration	239	7.1
T6	Tempursari	Line4:1400m	Andesite	Py disseminated	566	12.4
T7	Tempursari	Line5:0m	Andesite	Non alteration	142	22.8

The result of laboratory test shows that rocks in the survey areas generally have the resistivity of a few hundreds ohm-m and the chargeability of 10 to 20 mV/V. The contrast of these properties appears to be mainly dependent on the degree of alterations (silicification, argillization etc.) and pyrite dissemination.

2 - 3 - 4 Discussion

(1) Resistivity and Chargeability Features

The laboratory test results and geological information led to the following resistivity and chargeability features regarding the rocks and geological structure in the survey areas.

(a) Resistivity

The rocks in the survey areas excepting limestone generally have resistivities of a few hundreds ohm-m, and there are not characteristic contrasts of the resistivity between the kinds of rocks. Limestone shows high resistivity of the order of 1,000 ohm-m and silicification will make the resistivity higher. Argillized zone and weathered zone could form low resistivity zone.

(b) Chargeability

The result of laboratory test shows that the background value of chargeability of the survey areas is relatively high at 10 to 20 mV/V. Limestone shows low chargeability less than 10 mV/V and silicification will make the chargeability lower. Pyrite disseminated zone and argillized zone would cause strong chargeability anomaly.

(2) Relation of IP Survey Results to Geological Structure and Mineralization

On the basis of the above features, the relation of the IP survey results to geological structure and mineralization is discussed below.

(a) Relation to Geological Structure

Rocks in the Seweden district would be widely altered because the low resistivities of the order of 10 ohm-m distribute throughout almost whole area.

(b) Relation to Mineralization

Fig. 3-25 shows chargeability anomalies on SL -100 m in the Seweden district and Fig. 3-26 shows those on SL 400 m in the Tempursari district. In these maps, the three strong chargeability anomalous zones were extracted around station 2400 and station 3200 m of line-3 in Seweden, and around station 600 of line-2 in Tempursari (hereinafter called SW3-2400, SW3-3200 and TM2-600 respectively). The features of these anomalous zones are as follows.

SW3-2400: low resistivity (50~100 ohm-m)
N-S direction
SW3-3200: low resistivity (20~50 ohm-m)
N-S direction
TM2-600: high resistivity (more than 200 ohm-m)
E-W direction
vertical structure

According to the geological survey, wide spread white-colored argillization and pyrite dissemination are observed in the Seweden district. Silicification and argillization are particularly strong in the dacite intrusive bodies and their vicinity in the Putih River Basin where copper and gold mineralization is observed. Therefore anomalous zones of SW3-2400 and SW3-3200 would indicate that argillized zones with pyrite dissemination are developed in the deep because of their high chargeability and low resistivity.

In the Tempursari district, Pyrite dissemination and alteration such as sericite are widely developed in Tertiary volcanic • volocanilastic rocks and intruding dioritic rocks. Gold, silver, copper mineralization is observed in parts of these alteration zones. Therefore Anomalous zone of TM2-600 would reflect pyrite dissemination in intruding rocks and silicified vein zones because of its high chargeability, high resistivity and vertical structure.

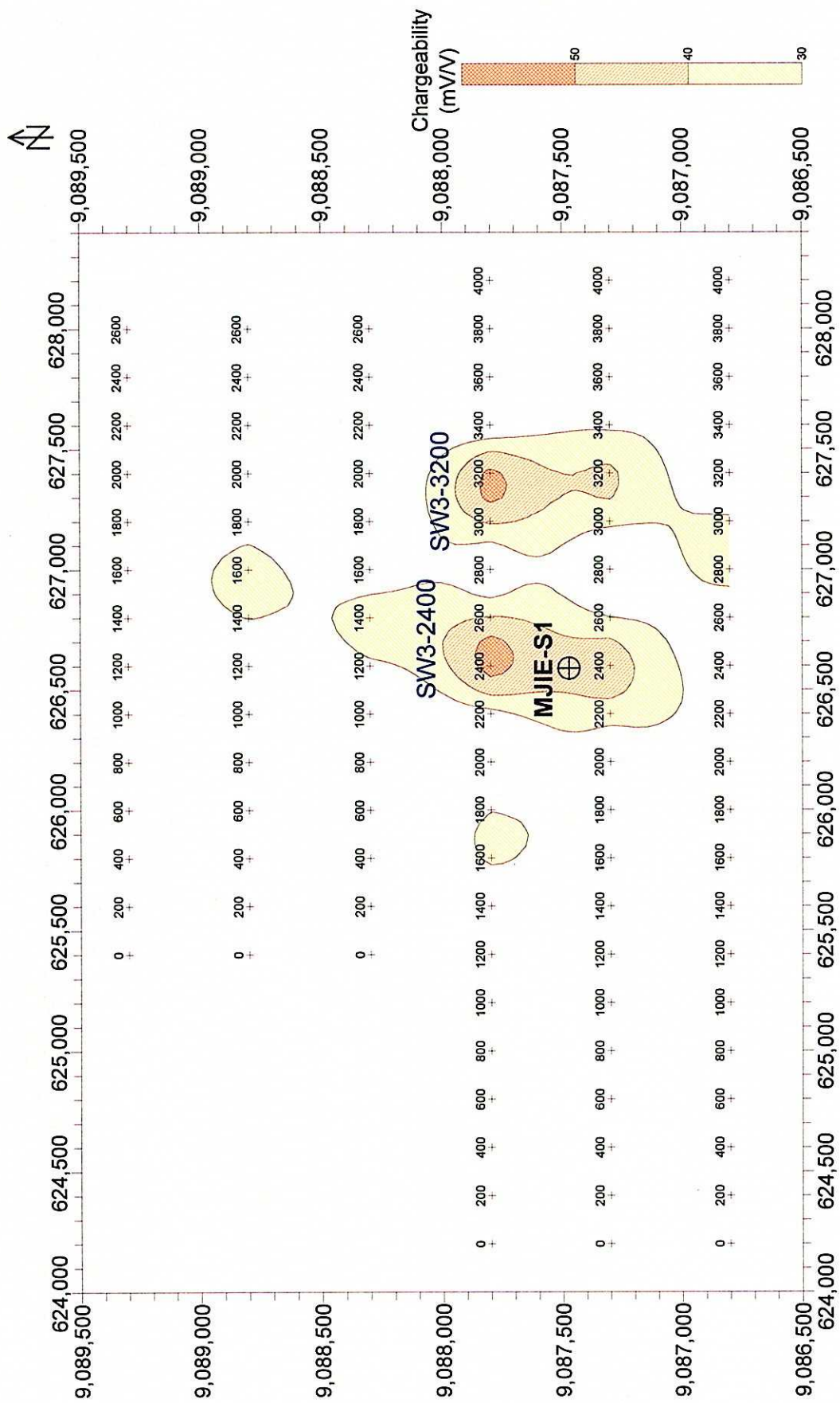


Fig.3-25 Geophysical Anomaly Map of the Seweden District

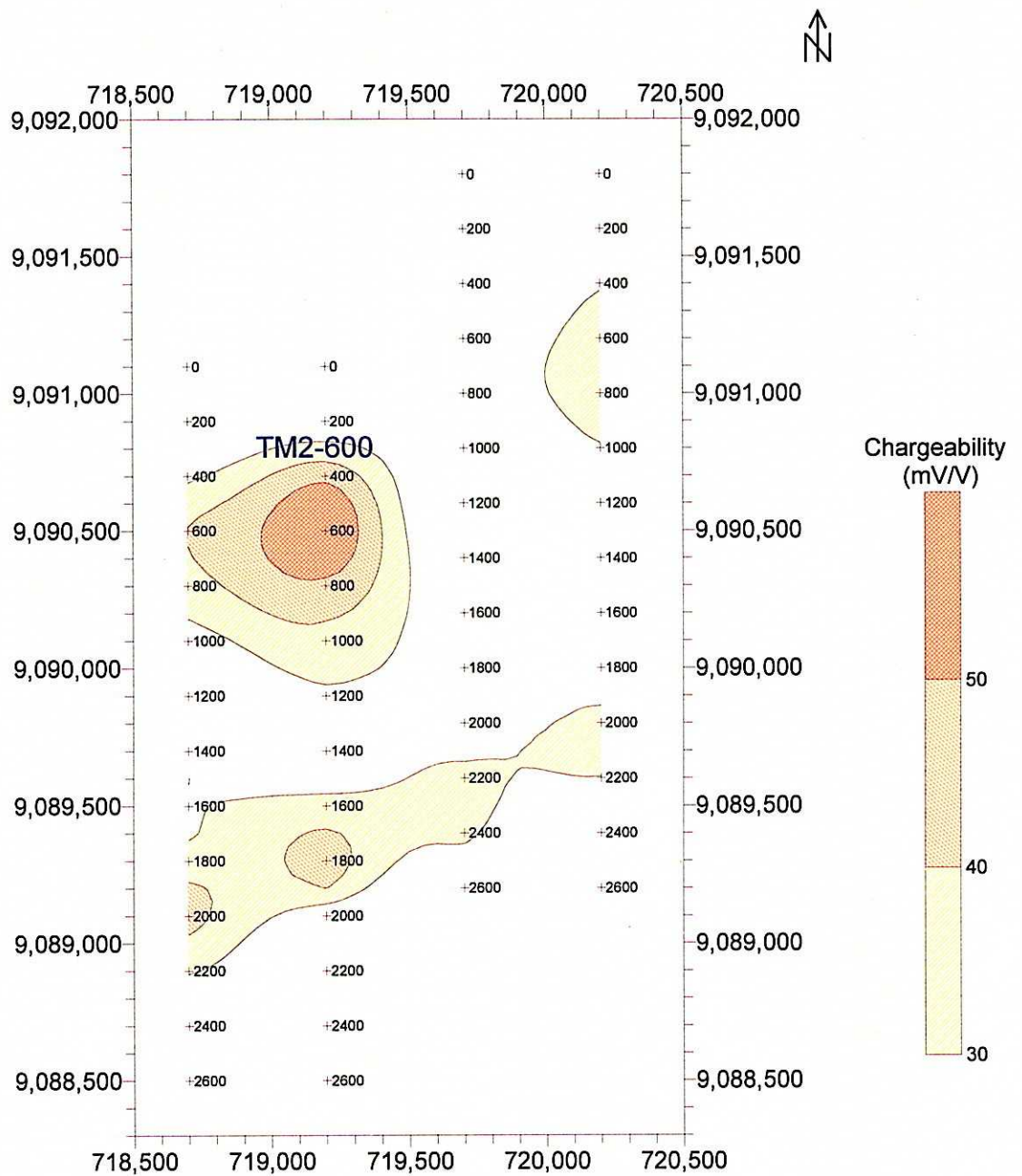


Fig.3-26 Geophysical Anomaly Map of the Tempursari District